Univerzita Karlova v Praze

Přírodovědecká fakulta

University of Aveiro

Department of Geosciences

Studijní program: Aplikovaná geologie

Studijní obor: Aplikovaná geologie se zaměřeními

RNDr. František Mantlík

Komplexní interpretace gravimetrických dat zaměřená na stanovení tektonické struktury a ekologické projekty

Complex interpretation of gravity data focused on tectonic structure assessment and environmental projects

Disertační práce

Školitelé: *RNDr. Miroslav Kobr, CSc.*

Prof. Manuel João Senos Matias

Praha 2013

Prohlášení

Prohlašuji, že jsem tuto práci vypracoval samostatně.

Všechny použité zdroje a materiály byly řádně citovány.

Práce nebyla využita jako závěrečná práce k získání jiného nebo obdobného druhu vysokoškolské kvalifikace.

V Praze dne

RNDr. František Mantlík

Table of Contents

Abstract

Gravimetry is an enormously expanding geophysical exploration method during the last decade. Unfortunately the gravity inversion ambiguity problem introduces the necessity to constrain gravity model parameters by other independent data.

Overview of gravity data processing and interpretation is presented. All stages of the project lifecycle are discussed with emphasis to the methodological aspects and new challenges introduced by common use of modern digital zero-length spring gravimeters. Special attention is drawn on approaches used in the presented case histories projects.

Description of the interpretation stage of the project concentrates on constraining of gravity model parameters with a complex of geophysical and geological data in order to reduce ambiguity of the inversion process in gravimetry. In addition, approaches used for delineation of tectonic structures, an important aspect of the interpretation stage, are described.

Three case histories examples are presented to demonstrate methodological aspects of the interpretation of gravity data. They are focused on environmental problems and tectonic structure assessment. The first project represents an attempt to use micro-gravity for determination of internal structure of an undocumented sealed landfill. The second project demonstrates interpretation of gravity data in complex with other geophysical methods for determination of prospective zones for possible future geothermal exploitation for production of electricity. Finally, the last project represents a regional study of the detailed structure of a sedimentary basin.

The projects presented provide practical demonstration of methodological approaches suitable for resolution of wide range of both environmental and tectonic structure problems.

Abstrakt

V posledních deseti letech představuje gravimetrie jednu z nejrychleji se rozvíjejících metod průzkumu v užité geofyzice. Problém nestability obrácené úlohy v gravimetrii však bohužel vede k nutnosti omezit parametry gravimetrického modelu pomocí nezávislých dat.

Práce přináší přehled zpracování a interpretace gravimetrických dat ve všech stádiích zpracování projektu s důrazem na metodologické aspekty a nové výzvy, které přináší širší rozšíření moderních digitálních gravimetrů založených na principu auto kompenzace. Zvláštní pozornost je věnována metodám použitým v prezentovaných případových studiích.

Popis interpretačního procesu je zaměřen především na postupy omezování nestability obrácené úlohy v gravimetrii omezením rozsahu parametrů modelu pomocí dostupných geologických a geofyzikálních dat. Kromě toho jsou popsány metody použité pro vymezení průběhu tektonických struktur, které tvoří důležitou součást interpretačního procesu.

Ve druhé části práce jsou prezentovány tři případové studie, které demonstrují popsané metodologické aspekty interpretace gravimetrických dat v praxi. Tyto studie jsou zaměřeny na úlohy v oblasti životního prostředí a určení tektonické stavby. První projekt představuje pokus o použití mikro-gravimetrie pro stanovení vnitřní struktury komunální skládky, která byla v minulosti zakryta bez pořízení detailní dokumentace. Druhý projekt ukazuje možnosti interpretace gravimetrických dat společně s komplexem dalších geofyzikálních metod pro stanovení perspektivních zón možného budoucího využití geotermální energie pro výrobu elektřiny. Poslední projekt je regionální studii detailní struktury sedimentární pánve.

Prezentované projekty představují praktické ukázky metodologických přístupů vhodných pro řešení širokého okruhu problémů tektonické stavby a ochrany životního prostředí.

1 Introduction

The aim of this dissertation is to present methodological aspects of the interpretation of gravimetric data with focus on the environmental projects and tectonic structure assessment. In three presented case histories, example surveys are described and methodological approaches used are presented and discussed. Special attention is drawn to the interpretation constrains based on using other geophysical and geological information. As a result, interpreted gravity models behave as complex interpretation models describing given problem from all known aspects.

Three case study examples represent a wide range of environmental and structural problems. In addition, they can be easily extrapolated to cover similar tasks related to other groups of challenges in applied geology.

In Chapter 2 of this Dissertation, overview of the gravity data processing and interpretation methods is presented. Procedures described in this Chapter were used for processing of gravity data in the case examples as presented. Important methodological notes concerning the use of modern digital gravity meters are based on the author’s experience with the processing of data from a wide range of projects including case examples as presented and supported by referenced resources.

Chapter 3 presents the case examples which were carried out as part of the author’s doctoral studies. Three projects are presented; two of them were realized in the Department of Geosciences of the University of Aveiro, Portugal while the third project was set up in the Czech Republic.

The first project represents a methodological study on a microgravity problem concerning landfill internal structure determination. The second project provides interpretation of the gravity data together with other geophysical methods for determining prospective zones for possible further hydrothermal exploitation for the production of electricity. Finally, the third project introduces re-interpretation of older regional gravity data in order to determine the detailed density distribution model of a sedimentary basin and tectonic structures buried under the sedimentary coverage of the basin.

Four appendices are attached to the Dissertation.

The Appendices A, B and C are full text versions of articles which present the case examples as given.

Appendix D is the description of the software for processing gravity data. The author of this dissertation created the software. It is currently in the production stage and is widely used for processing gravity projects around the world including those presented in this Dissertation.

Acknowledgements

The author would like to acknowledge first of all the great support, help and understanding from both supervisors, RNDr. Miroslav Kobr, CSc., and Prof. Manuel Joao Senos Matias.

This dissertation could not be completed without outstanding support from the University of Aveiro, Department of Geosciences and Geonika company, Prague.

Special thanks have to be expressed to the EU Erasmus project.

Last but not least the author would like to express his grateful thanks to everybody who was involved in the process of creating this dissertation and in the projects presented.

2 Overview of gravity data acquisition and processing

Enormous expansion of the use of gravimetry for many applications of applied geophysics can be seen during the last decade. Administrative restrictions for gravity surveys were left out in most countries. In addition, the shortage of precise field gravimeters nearly came to an end. For example, the Canadian producer of field digital zero-length spring gravimeters suitable for applications in applied geophysics Scintrex Ltd. announced the delivery of as many as 1,000 CG-5 gravimeters in the last 10 years *(Scintrex 2012)*.

In addition, many software packages for gravity data processing and interpretation were introduced *(e.g. Geosoft 2010; Mantlík 2013)*. It made the post-acquisition stage of gravity surveys cheaper and faster.

All the above aspects lead to the increasing popularity of gravity methods in environmental and engineering applications.

In general, gravimetry provides the following important advantages compared with other commonly used geophysical methods:

- The potential field nature of the gravity field. Sources of gravity anomalies are characterized by a precisely defined physical quantity, i.e. density of anomalous rock media.
- Theoretically unlimited vertical reach. The only limitations are the horizontal extent of the survey and attenuation of the gravity signal proportional to the square of the distance to the source.
- Limited and well defined sources of noise. Most of the survey noise can be excluded in the pre-processing or processing stage. This fact makes gravity information highly reliable in most situations.

On the other hand, the following limiting factors have to be taken into account:

- The ambiguity of gravity models. An infinite number of gravity models can be constructed and each of them will fit the given gravity anomaly perfectly. Additional geological and/or geophysical information is always needed to constrain gravity models.

- Strong attenuation of the gravity signal. This is the most important limiting factor for vertical reach of any gravity survey. Very large targets with strong density contrast can be detected while a signal from other deep targets remains undetectable.

- Low production speed. Comparing to other geophysical methods, gravimetry is a relatively complicated method from the point of view of survey logistics among others because of the need of an accompanying precise topographic survey. In addition, collecting gravity data in the field is a slow process comparing to e.g. magnetometry.

- Survey cost. Both equipment cost and the relatively expensive field survey procedure are additional limiting factors in the further expansion of gravimetry.

It can be concluded from the above lists, that in addition to the gravity data acquisition and the accompanying high-precision topographic survey, additional constraining data should be collected, processed and interpreted. The case examples presented in this Dissertation show typical usages of this complex approach in real situations of typical environmental and structural studies.

This Dissertation is focused on land gravity data acquisition and processing only. Marine and airborne applications are not discussed here.

2.1 Field data acquisition and reductions

A gravimetric field survey lifecycle consists of the following stages:

- Survey planning stage

- Data acquisition stage
- Data reductions and processing stage.

2.1.1 Survey planning stage

In the survey planning stage, data collecting strategy is established. In addition to the survey geometry definition, selection of geophysical methods for the survey is established. In case of a gravimetry survey, the selection of accompanying constraining methods is a key task.

Typically, methods based on completely different physical principles are suitable candidates for constraining gravity data. In the case studies presented in this Dissertation, electrical resistivity methods and reflection seismics are the most commonly used methods. Both of them are able to provide results which are not directly related to the density distribution pattern and as such can support gravity models with independent constrains.

As mentioned earlier, the gravity data acquisition stage is always accompanied with the precise geodetic survey. Accuracy of the geodetic survey, mainly the accuracy of the stations elevation data, is the key factor influencing overall precision of the gravity survey especially in case of low-scale microgravity projects. Carefully operated modern digital relative field gravimeters can provide reliable gravity data with precision better than 0.005 mGal *(Scintrex 2012b p. 6-2)*. Because topographic data acquisition is completely independent from the gravity survey and the topographic survey results are used for computation of gravity reductions used in the data processing stage, overall uncertainty of the processed results can be expressed as the sum of uncertainties for both gravity survey and topographic survey.

Vertical gradient of the gravitational field on the Earth's surface is approximately 0.2 mGal.m^{-1} *(Formulas 2.5, 2.8 and 2.9)*. Thus, in order to get precision of the station elevation assessment comparable to the uncertainty in gravity values estimations, topographic survey vertical error should be lower than approx. 25 mm. This level of accuracy cannot be achieved with common tools like a handheld GPS instrument or an interpolation of stations elevations from a digital terrain model (DTM). Special equipment, e.g. a geodetic differential GPS (DGPS) system or geodetic total station/optical leveling instrument accompanied by corresponding processing tools have to be used.

2.1.2 Data acquisition stage

The key problem concerning gravity data acquisition is the establishing of procedures for determining and eliminating the instrument drift effect. The approach for drift determination has rapidly changed with the introduction of digital instruments equipped with capacitance based auto-compensation mechanism.

Older mechanical instruments (e.g. Lacoste & Romberg Micro G gravimeter) equipped with zero-length spring sensor system used mechanical lock system of the sensor when the instrument was not in operation. Thus the spring was under no tension between survey days or when the instrument was carried between stations. Because of this, mechanical properties of the spring inside the sensor were not changing significantly with time and the long-term drift of the instrument was very low, most often significantly lower than 0.1 $mGal.day^{-1}$. Any higher drift value indicated problems caused most likely by untidy operation, inner temperature instability, or instrument malfunction.

On the other hand, sensors of the modern digital instruments are constructed differently. The sensor system is kept in a fixed position with the use of the auto-compensation system which is based on capacitance principle. Thus, the spring is under perpetual tension during the whole life span of the instrument and the sensor is never locked, or, in other words, it is permanently locked in a permanent state of tension. Because of this constructional difference, mechanical properties of the spring inside the sensor are changing with time due to natural relaxation of the spring. This leads to a significant nearly linear instrument drift effect which is typically in the range between 0.5 – 1.5 $mGal.day^{-1}$, i.e. nearly two orders higher than is the case with older instruments. The most significant part of this drift effect is cleared inside the instrument processing software (firmware). Nevertheless, the residual part of the instrument drift is always registered and has to be cleared from the data later in the processing stage *(Scintrex 2012b p. A-16)*.

Thus, while the indicator of the inner stability of older mechanical instruments was the low values of instrument drift for every survey day, in the case of digital gravimeters the important indicator of stability is linearity of the instrument drift during the survey loop while the absolute value of this linear drift is not important.

As a general consideration, regardless of the type of gravimeter used, determination of the temporal development of the instrument drift effect is an important precaution for the decision of selected gravity survey strategy.

Depending on the required precision of the survey, instrument drift is either established based on the reading at a gravity base at the beginning and end of each survey day (gravity loop), either a gravity base is visited in regular intervals during the survey day in order to provide piecewise check of the instrument drift development during the day. More advanced post-processing systems are capable of determining instrument drift temporal development not only from the repeats at the dedicated base station, but every repeated reading at an arbitrary gravity station during the day can become part of the drift development assessment *process (Mantlík 2013 p. 45)*.

In either case, in addition to the in-loop repeats for instrument drift determination described above, overall survey precision has to be checked by a set of cross-loop repeats, i.e. independent occupations of selected stations in successive daily loops. Thus, the quality of the data acquisition and the primary processing including the uncertainty caused by instrument drift disturbances can be reliably determined.

2.1.3 Gravity data processing stage

The goal of primary gravity data processing stage, often called data reduction stage, is to clear the raw data from the known sources of temporal and spatial disturbances not connected to the sources of gravity field under study. Not all processing steps (data reductions) are implemented for each type of gravity survey. Selection of required reductions represents an important consideration in the survey preparation stage.

Table 2.1 summarizes reductions used in gravity survey processing.

Gravity reduction	*Typical range [mGal]*	*Note*
Instrument drift correction	0 – 0.050 / 0 – 0.010	1)
Tidal correction	-0.200 – 0.200	2)
Latitude correction (theoretical gravity)	< 8,000	
Eötvös correction	n/a	3)
Free air correction	n/a	
Bouguer correction	n/a	
Terrain correction	always < 0	
Isostatic correction	n/a	4)

Table 2.1. Summary of gravity reductions.

Notes:

1) – first range represents typical drift values interval for mechanical gravity meters, second range is expected drift linearity for digital instruments.

2) – for micro-gravity surveys is often incorporated into drift correction.

3) – used for airborne and seaborne surveys only.

4) – used for continental-scale surveys only.

Instrument drift correction clears each gravity observation from the effect of instrument drift. At the stage of instrument drift development assessment, quality of the survey based on cross-loop repeats can be estimated as discussed in detail in the previous section.

Effects of gravity changes caused by attraction of Moon, Sun and planets are cleared by the **tidal correction**. Typical amplitude of tidal correction is +/- 0.2 mGal. Tidal effect temporal development at the Earth's surface is well described *(e.g. Doodson 1921; Cartwright and Tayler 1971; Cartwright and Edden 1973; Tamura 1987)* and can be computed with high precision, in most cases better than 0.001 mGal. On the other hand, formulas for tidal effect computation are complex and can't be easily incorporated e.g. into a spreadsheet form. Tidal effects temporal development is smooth with major period of 12 hours; therefore micro-gravity surveys with sufficient number of repetitions (at least every 2 hours) often incorporate tidal effects as a part of instrument drift correction.

Digital gravimeters have a simpler formula for approximate calculation of tidal effects built in their firmware, so that the output value from the instrument can be corrected for tidal effect automatically. Tidal correction computed according to this formula *(Longman 1959)* can differ from the correct value for more than 0.005 mGal under some circumstances. In addition, a fixed station position is used for tidal effects calculation which can cause additional uncertainty especially for large regional surveys. Because of these problems, newest gravity processing software packages clear the raw data from the tidal correction computed inside the gravimeter and provide correction based on precise computations instead *(e.g. Mantlík 2013; Geosoft 2010)*.

Gravity value obtained from the relative gravimeter corrected for instrument drift and tidal effects represents a relative gravity acceleration which is constant for a given station and instrument. When absolute gravity value is known for at least a single station in the survey, absolute gravity for each station can be easily computed from the difference between relative gravity values of the current station and the station with known absolute gravity.

Ellipsoidal approximation of the Earth's shape well known from geodesy is used in gravimetry as well. Vertical component of a vector sum of the gravity acceleration caused by the Earth's mass at the ellipsoid level and the centrifugal acceleration caused by Earth's rotation provides the value of **theoretical gravity** or **normal gravity**, which is a subject of international standardization. The most commonly used theoretical gravity formulas are IGF 1930 formula:

$$g_0 = 978049\,.\,(1 + 0.0052884\, sin^2\, \lambda - 0.0000059\, sin^2\, 2\lambda) \qquad \textit{(2.1),}$$

the IGRS 1967 formula:

$$g_0 = 978031.846\,.\,(1 + 0.0053024\, sin^2\, \lambda - 0.0000058\, sin^2\, 2\lambda) \qquad \textit{(2.2),}$$

and the GRS 1980 formula:

$$g_0 = 978032.67714 \frac{1+0.00193185138639 \sin^2 \lambda}{\sqrt{1-0.00669437999013 \sin^2 \lambda}} \qquad (2.3)$$

All gravity accelerations are in mGal.

Gravity values computed according to the 1930 formula can differ from values from other formulas by as much as 17 mGal *(Blakely 1995 p. 135-136)*.

Reduction of absolute gravity value at a gravity station for the influence of theoretical gravity is often called **latitude correction**.

In case of gravity readings made by moving instruments, e.g. in case of airborne or seaborne survey, additional centrifugal force is generated due to the movement. Correction for this influence is called **Eötvös correction** and is not applicable in a typical ground survey.

Free air correction is used to eliminate influence of vertical gradient of the Earth's gravity field. The free air correction g_a is computed according to the formula

$$g_a = -\frac{2 . g_R}{R} . h \qquad (2.4)$$

where g_R represents gravity value at sea level, R diameter of the Earth and h elevation above sea level *(Blakely 1995, p. 140)*. Thus, expressed in units of mGal (10^{-5} m.s^{-1}):

$$g_a = -\, 0.3086 . h \qquad (2.5)$$

for h in meters.

Absolute gravity value for a station g corrected for both latitude and free air correction is called the **free air anomaly** g_F:

$$g_F = g - g_0 - g_a \qquad (2.6)$$

Free Air correction takes into account Earth's body masses up to sea level (geoid) only. Any exceeding material between the geoid level and the Earth's surface where the gravity station is sited are omitted. To compensate for these exceeding materials, **Bouguer correction** is introduced. Assuming ρ as average density of the rock material between sea level and station elevation, Bouguer correction g_b can be computed according to the formula

$$g_b = 2\,\pi\,\gamma\,\rho\,h \tag{2.7}$$

where γ represents Newton's gravitational constant.

For average density of the upper part of the Earth's crust 2.67 $g.cm^{-3}$ the Bouguer correction in mGal becomes

$$g_b = 0.1119\,.\,h \tag{2.8}$$

When Bouguer correction is applied to the free air anomaly value, the resulting gravity value is called **Bouguer anomaly** g_B:

$$g_B = g_F - g_b \tag{2.9}$$

(Blakely 1995 p. 143)

Bouguer correction compensates influence of the geological material between geoid and station elevation as a homogenous infinite horizontal slab. It does not take into account differences caused by terrain irregularities, i.e. exceeding mass in case of hills above the station elevation and deficiency of mass in valleys and similar structures below the station. **Terrain corrections** reduce gravity readings from terrain effect.

It is evident that any terrain irregularity, positive or negative, causes decrease of gravity measured at a station. That means that if we apply the convention similar to other gravity reductions, that a correction has to be subtracted from the uncorrected value; terrain correction is always negative, i.e. increasing the gravity value for the value of compensation needed.

Computation of terrain corrections is a time and resources consuming task. Usually, digital terrain model is used to obtain terrain shape in the surroundings of the survey area. The gravity effects caused by exceeding and missing masses are modeled by the effects of suitable simple geometric bodies. The influences of the masses of all the bodies on the gravity field at the station are summarized in the total terrain correction. The procedure is repeated for every station.

The classical approach for terrain corrections computation models the gravity influence of the terrain by concentric cylindrical segments divided into directional zones called Hammer's method *(Hammer 1939)*.

Table 2.2 presents definitions of the Hammer's zones and the numbers of segments in each zone. The diameters of the zones and the numbers of the segments are chosen so that the influence of every segment on the total value of the correction is similar to the influence of any other segment, i.e. taking into account attenuation of the gravity signal with the square of the distance.

Zone	**A**	**B**	**C**	**D**	**E**	**F**	**G**
# of segments	1	4	6	6	8	8	12
Outer radius [m]	2.0	16.6	53.3	170.1	390.1	894.8	1529.4
Zone	**H**	**I**	**J**	**K**	**L**	**M**	
# of segments	12	12	16	16	16	16	
Outer radius [m]	2614.4	4468.8	6652.2	9902.5	14740.9	21943.3	

Table 2.2: Hammer method – number of segments and outer radius for each zone. Zone A represents a full cylinder of a radius of 2 meters.

Influence of an individual Hammer's segment g_{tH} can be determined by the formula:

$$g_{tH} = -\frac{2\pi.\gamma.\rho}{N}\left(r_2 - r_1 + \sqrt{r_1^2 + h^2} - \sqrt{r_2^2 + h^2}\right) \tag{2.10}$$

where r_1 and r_2 are inner resp. outer radius of the zone, N is the number of segments and h is the elevation difference between the station and the average elevation of the area inside the segment.

Terrain corrections based on Hammer's method used to be computed manually with the help of detailed paper topographic maps and template transparencies with the segments chart. Modern gravity processing software provides automatic fitting of available digital terrain model data into the segments and fully automated terrain corrections computation *(Mantlík 2013)*.

With the expansion of computers and the wider availability of digitized terrain data, more straightforward methods dedicated to computerization were developed. The method published by *Plouff (1976)* models each individual cell of a digital terrain model with the help of a vertical rectangular prism. The gravity effect of the prism g_{tP} can be computed using the formula:

$$g_{tP} = -\gamma.\rho \sum_{i=1}^{2}\sum_{j=1}^{2}\sum_{k=1}^{2} \mu_{ijk} \left(z_k \tan^{-1}\left(\frac{x_i.y_j}{z_k.R_{ijk}}\right) - x_i.log\left(R_{ijk} + y_j\right) - y_j\,.log\left(R_{ijk} + x_i\right) \right)$$

where

$$R_{ijk} = \sqrt{x_i^2 + y_j^2 + z_k^2}\,, \quad \mu_{ijk} = (-1)^i\,.(-1)^j\,.(-1)^k \qquad \textit{(2.11)}$$

Terrain corrections computation procedure based on Plouff' method is included e.g. in *Mantlík (2013)*. One of the important advantages of this method compared to the classical Hammer approach is its easy expansion over the limit of 22 km from the station which is important for larger regional surveys.

Density ρ used in Formulas 2.7, 2.10 and 2.11 is called **reduction density**. In most applications, a constant value of reduction density is used for the computation of both Bouguer corrections and terrain corrections. Mean value of density of rocks available in the survey area should be used. Usually, if there is no information concerning geological situation and rock densities available, the value of 2.67 $g.cm^{-3}$, representing average density of the upper part of the Earth's crust can be used.

Density values determined from rock samples in the laboratory can provide more reliable estimate of reduction density. Nevertheless, the values of rock sample densities from the laboratory can be lower than the in-situ densities of the same rock by as much as up to 5 percent. It depends on the type and condition of the rock because of the lack of pressure from the upper layers under lab conditions. There is also a density decrease possible because of the change in the content of water in the sample and because of other influences *(Tsirel 1994)*.

Another approach is to determine the density of the rocks from the gravity data. The commonly used method was introduced in graphical form by *Nettletton (1942)* and switched to analytical form by *Jung (1953)*. The principle of the method is simple. Complete Bouguer anomaly over a profile with significant elevation differences is computed for a set of different reduction densities and gravity vs. elevation plot is made for each density. The worst correlation result between gravity and elevation corresponds to the best fit of reduction density.

Jung's modification of Nettletton's method introduces the possibility to compute the optimal reduction density ρ_n directly based on the series of gravity observations g_i, corresponding elevations h_i and reduction density ρ used for computing g_i values:

$$\rho_n = \rho + \frac{\sum_{i=1}^{n}(g_i - \bar{g}) \,.\, (h_i - \bar{h})}{2 \,.\, 10^8 \,.\, \pi \,.\gamma \sum_{i=1}^{n}(h_i - \bar{h})^2} \qquad (2.12)$$

Gravity values are in mGal, elevations in meters and densities in $g.cm^{-3}$, $\bar{h}$ and $\bar{g}$ represent average elevation and gravity for the whole series respectively. Formula 2.12 can be used iteratively to fine-tune the estimation (Jung 1953).

Complete Bouguer anomaly data used for density determination must be cleared from any trend caused by deeper sources. Otherwise computed reduction density can be significantly influenced by the trend and the result can be wrong.

Finally, **isostatic correction** provides correction for regional effect of isostasy, i.e. effect of auto-compensation of large-scale mass excesses in high mountain regions and deficiencies in ocean areas for continental-scale surveys.

Bouguer anomaly value corrected for terrain influence g_t is called **Complete Bouguer anomaly** g_C:

$$g_C = g_B - g_t \tag{2.13}$$

Complete Bouguer anomaly is usually the final product of the basic gravity survey processing. Gravity field represented by the Complete Bouguer anomaly is cleared from all known disturbances which are not caused by lateral density changes below the surface. That means that positive anomalies of the Complete Bouguer field represent indicators of presence of higher density sources while negative anomalies can indicate cavities or the presence of material with lower density compared to the reduction density used.

In addition to the qualitative interpretation based on assumptions presented above, complete Bouguer anomaly field serves often as input information for further post-processing and gravity modeling/inversion quantitative interpretation phase described in the following chapters.

2.2 Post-processing and transformations

Post-processing stage of the gravity survey is the stage of cleaning and fine-tuning of the survey data. Secondary products are derived from the measured field from various points of view trying to emphasize aspects of the data important for interpretation.

The most common procedures used in the post-processing stage of survey lifecycle are regional and local field separation and various field transformations.

2.2.1 Regional field separation

As the first step when all acquired data are processed and the final version of the complete Bouguer anomaly field is available, separation of the influence of the regional field caused by distant sources out of the scope of interest takes place.

Depending on the survey extent, the density of stations and other factors, the following methods are most frequently used for regional field assessment and separation:

- Fitting of the regional field trend from general trends in survey data;
- Determination of the character of regional field from a special small survey which significantly extends boundaries of the area of interest;
- Assessment of the regional field from the known/estimated behavior of the regional field sources.

The first method, **fitting of the regional field trend**, represents the most common approach for small-size micro-gravity surveys but is not limited to them. The regional field is modeled by a simple function, e.g. linear or polynomial for profile data resp. planar or bicubic for 2-dimensional data. The function parameters are usually obtained with the least square fitting. In the case study example presented in Appendix C, bilinear and bicubic regional field fitting is presented *(Mantlík and Matias 2010 p. 825-826)*.

The regional field fitting from survey data can be problematic under some circumstances. Particularly, if the survey area is limited to a strong local anomaly, the shape and position of the anomaly can influence the fitting process strongly. Similarly, a very small survey area with a strongly varying local field can have the same effect. The second method, **a dedicated regional field fitting survey**, can solve such problems.

For a single profile survey, the profile is often extended with significantly higher station spacing. The extension is used to fit the regional field. Similarly, in case of a grid survey, the central profile or several selected profiles are extended in a similar way.

Less frequently, other strategies for regional field determination are used. E.g. for a case study presented in Appendix A, a dedicated profile parallel to the micro-gravity survey profile sufficiently far from the influence of the expected target was established *(Mantlík et al. 2009 p. 358)*.

The third possible approach is to **assess the regional field properties with the use of a regional gravity model** constructed from known geological and geophysical data. E.g. a regional scale gravity survey interpretation model can be used to assess the regional field shape for a detailed local survey. A similar approach was used in case studies presented in Appendix B e.g. in the Nová Paka locality *(Mantlík and Karous 2013)*.

As a result of subtraction of the regional field from the complete Bouguer field, a **residual gravity field** is computed. From the point of view of interpretation, the residual field anomalies represent the influence of individual local targets of interest for the given survey while the influence of large-scale targets is removed.

For example, in the Aveiro Basin case study example presented in Appendix C, both complete Bouguer field and the residual field take place in the interpretation. The Complete Bouguer field is used to model the overall sedimentary basin shape and spatial development of basin depth while detailed structural features is suppressed. On the other hand, the residual field provides details of all the detectable structural elements while the influence of the overall shape of the basin is suppressed *(Mantlík and Matias 2010)*.

2.2.2 Transformations

The potential field nature of the gravity field provides more possibilities for data enhancement and for emphasizing features important for further interpretation. Visual presentation of the transformed fields can help with qualitative delineation of structural features as well as with distinguishing between individual targets.

The most commonly used transformations of the two-dimensional representation of the gravity field are:

- Directional gradients of the gravity field
- Total horizontal gradient
- Vertical derivatives
- Vertical continuation (upward, downward).

Directional gradient magnitude of the gravity field can be computed as an estimate of the value of corresponding derivative of the gravity field in the particular direction. After *Blakely (1995, p. 324)*, for the planar distribution of gravity field g(x,y) uniformly sampled in the x direction with the sampling interval Δx, the directional derivative at the location with coordinates x_i and y_i can be estimated using the formula:

$$\frac{dg(x_i,y_i)}{dx} \cong \frac{g(x_{i+1},y_j)-g(x_{i-1},y_j)}{2.\Delta x} = \Delta g_x(x_i,y_j) \qquad (2.14)$$

Similarly, directional gradient in the y direction can be estimated as:

$$\frac{dg(x_i,y_i)}{dy} \cong \frac{g(x_i,y_{j+1})-g(x_i,y_{j-1})}{2.\Delta y} = \Delta g_y(x_i,y_j) \qquad (2.15)$$

Examples of usage of directional gradient for interpretation of structural features are presented in Appendix C *(Mantlík and Matias 2010 p. 829)*.

Total horizontal gradient magnitude can be estimated using the formula (after Blakely 2005 p. 348):

$$\Delta g_H = \sqrt{\Delta g_x^2 + \Delta g_y^2} \qquad (2.16)$$

Total horizontal gradient tends to have maxima located at density interfaces. This behavior can be used for automatic detection of linear structures indicators. Algorithms scanning the horizontal gradient field and fitting local extremes were developed *(e.g. Blakely and Simpson 1986)*.

As a replacement for the simplistic approach for computation of directionally independent indicator of lateral changes of the potential field, higher order vertical derivatives can be used. For example, the second vertical derivative can be expressed as the direct consequence of the Laplace's equation for the potential field ϕ *(after Blakely 1995 p. 325)*:

$$\nabla^2\Phi = 0\,, thus\ \frac{\delta^2\Phi}{\delta z^2} = -\frac{\delta^2\Phi}{\delta x^2} - \frac{\delta^2\Phi}{\delta y^2} \qquad (2.17)$$

The Equation 2.17 can't in general be easily solved in the real domain, but it can be converted to the frequency domain:

$$F\left[\frac{\delta^2\Phi}{\delta z^2}\right] = k_x^2\, F[\Phi] + k_y^2\, F[\Phi] = |k|^2 . F[\Phi] \qquad (2.18)$$

where operator F[Φ] represents Fourier transform of Φ and k is wavenumber $k = {}^{2\pi}/_{\lambda}$, value of λ represents wavelength.

With the use of the Equation 2.18, second vertical derivative can easily be computed using the following procedure:

1) Transform the gravity field into Fourier domain. Numerical methods for multi-dimensional discrete Fourier transform can be used, e.g. *Press et al. (1986)*.
2) Multiply transformation result by $|k|^2$.
3) Transform the field back from the Fourier domain to the real domain.

It can be shown *(Blakely 1995 p. 326)* that nth-order vertical gradient can be computed as:

$$F\left[\frac{\delta^n \Phi}{\delta z^n}\right] = |k|^n . F[\Phi] \qquad (2.19)$$

Thus, computation of vertical derivative of any order can easily be made in the Fourier domain by adapting the above described procedure.

In addition to the presented computation in the frequency domain, formulas based on simplified models were developed, e.g. *Elkins (1951)*. The Elkins' formula computes the value of the second vertical derivative as a linear combination of gravity field value in a node of the rectangular grid under study and in the 16 surrounding nodes. In case of a noisy gravity field, Elkins' method can provide more stable result than the second vertical derivative computed in the Fourier domain *(Mantlík and Matias 2010 p. 828)*.

An example of using a second vertical derivative field for interpretation of presence of possible tectonic structures is shown in the Appendix C *(Mantlík and Matias 2010 p. 828-830)*.

Vertical continuation of the potential field is another transformation based on Laplace's equation consequences. If the distribution of the gravity field in a planar surface at the level z_0 is known, gravity field distribution at the planar surface parallel to the first one at the level $z_0 + \Delta z$ can be computed. The only condition is that all sources of the gravity field under study are located below both surfaces.

It can be shown *(Blakely 1995 p. 313-316)* that distribution of a potential field U at a level surface $z_0 + \Delta z$ can be expressed by a downward-continuation integral:

$$U(x, y, z + \Delta z) = -\frac{\Delta z}{2\pi} \iint_{-\infty}^{\infty} \frac{U(x', y', z_0)}{[(x - x')^2 + (y - y')^2, \Delta] z^2} \, dx' \, dy' \qquad (2.20)$$

Transformation of the Equation 2.20 into frequency domain gives:

$$F[U(x, y, z + \Delta z)] = e^{\Delta z \,.[k]} \,. F[U(x, y, z)] \qquad (2.21)$$

and for computation of vertically shifted field values the adapted procedure for computation of vertical derivatives can be used.

From the Equation 2.21 can be seen, that the **upward continuation** of the gravity field, i.e. continuation with Δz greater than zero behaves as the application of a low-pass filter to the original field. That means that long wavelength features are emphasized in favor of short wave phenomena. As such, upward continuation can be used for the filtering of noise data and for producing a general view of the survey area. In addition, significantly upward continued field can be used as a regional field and separated from the data as discussed in the previous chapter.

On the other hand, **downward continuation** behaves as a high-pass filter. Short wavelength structures are emphasized and become more pronounced in the continued field. Unfortunately, together with the useful signal, short period noise contained in the data is emphasized as well. If the downward transformation is not made with care, amplified noise can completely cover the useful signal.

In addition, the basic condition for the physical sense of the potential field transformation has to be met, i.e. the surface level of the downward continued data must not reach the gravity field sources. When the depth to the sources is reached, the downward continued field is obviously distorted.

Examples of the downward continued field can be found in the case study example presented in the Appendix C *(Mantlík and Matias 2010 p. 830-832)*.

2.3 Gravity models

The final stage in the gravity data processing and interpretation process is the construction of the interpretation models describing the properties of the environment under study which can explain the behavior of the collected data. In general, in geophysics, the automated process striving to construct a model which best fits measured data is called *forward problem*. The computation of values of a geophysical field from the known distribution of sources is called *inverse problem*.

Automatic forward problem solution of potential field data is strongly limited by ambiguity caused by the nature of the potential field. While the resulting potential field response to a given distribution of sources can be more or less easily computed and each sources configuration generates a unique potential field distribution, for a given distribution of potential field an infinite number of sources configurations perfectly fitting the field can be found. In addition, the fitting sources distributions can vary significantly.

For example, any homogenous sphere object of any diameter placed in a given center produces exactly the same gravity field supposing that the mass of each sphere is identical. As such, an assumption of the interpreter, that the source of the anomaly can have spherical shape is not sufficient to produce a reasonable model. Additional constraining information, such as the depth to the top of the anomalous body, density contrast etc. has to be provided.

Thus, the forward method of gravity modeling consists of the following steps:

1) Initial density distribution model is constructed based on known constraining data.
2) Based on the model, gravity anomaly is calculated.
3) Anomaly computed in the step 2) is compared to the observed anomaly.
4) Model parameters are adjusted to get next iteration closer to the observed data. Constraining information has to be taken into account to keep the model realistic.

Steps 2)-4) are repeated until the match between the observed and calculated anomaly reaches satisfactory level.

It can be concluded from the above that in the interpretation phase of a gravity project, independent information has to be available which can constrain assumptions for the gravity model. Because of that, no gravity model can be presented as a result of gravity data processing and interpretation only. Each gravity model is by its nature an interpretation model based on complex assessment of the available geological, geophysical and other related information.

The complexity of the construction of gravity models and need for evaluation of a wide range of resources is the reason why no fully automatized gravity inversion procedure is available. The inversion process always needs full attention of the interpreting geophysicist and often multidisciplinary co-operation is needed.

On the other hand, because of the complexity of preparation of a gravity interpretation model, the result obviously represents not only possible interpretation of the gravity field obtained in the survey area, but serves as a complex geological/geophysical interpretation model based on all available multidisciplinary data.

In the remaining part of this chapter, technical aspects of the gravity modeling are described. Practical aspects and case examples with the focus on the subject of this Dissertation are discussed in the following chapters.

2.3.1 Overview of gravity modeling methods

Computation of the gravity response of a given mass distribution is in theory a simple process. Gravimeters can measure vertical component of the gravity field, i.e. the gravity response g(x, y, z) corresponds to the vertical derivative of the spatial distribution of the gravity potential U:

$$g(x,y,z) = \frac{\delta U}{\delta z} = -\gamma \iiint \rho(x',y',z') \frac{(z-z')}{\sqrt{(x-x')^2+(y-y')^2+(z-z')^2}^{\,3}} \, dx'dy'dz' \tag{2.22}$$

The value of g is calculated for each required point with coordinates (x, y, z) by integrating over the spatial density distribution $\rho(x', y', z')$ *(after Blakely 1995 p. 185)*.

In practice, direct algebraic solution of the integral *2.22* is limited to simple geometrical objects with simple density distribution, e.g. homogenous or linear gradient model. On the other hand, because of the principle of superposition, gravity signals of small elementary objects can be summarized to obtain the total signal of a larger object consisting from these elements. While being computationally intensive, this approach can be afforded exploiting modern computers.

For example, real geological objects can be modeled with the rectangular prisms with sides parallel to the coordinate axes. The gravity response of an individual prism expressed as solution of the integral 2.22 was computed by *Plouff (1976)*. The result presented in *Formula 2.11* is used for modeling terrain corrections effect as discussed in Section 2.1.3 of this Dissertation.

2.3.2 2D gravity models

The need of constraining gravity models with independent data which in most cases cannot be automatized makes the modeling process extremely complex. Practical application of modeling procedures needs some level of simplification. The most common way of simplification is the reduction of dimensions of the model. In case of the 2D model, the full space model of the geological environment is replaced by its cross-section at the position of the profile under study. Unchanged cross-section structures continue on both sides of the profile.

Despite of the strange appearance of the idea of such brutish simplification, in many geological situations simplification of the three-dimensional complex geological setting with a 2D profile section is not only the domain of gravimetry. Geological cross-sections are of common use in many tasks. In addition, many geological objects running perpendicularly to the direction of profiles can be approximated with two-dimensional objects, i.e. objects with infinite extent on both sides of the profile, with a high level of precision. In most situations, the gravity signal from parts of the two-dimensional object which significantly exceed the profile extent is negligible and can be omitted.

E.g. *Peters (1949)* suggests considering a body to be two-dimensional when an extent of the anomaly of elliptical shape caused by the body perpendicular to the profile extends more than three-times the extent in the profile direction. Similarly, *Grant and West (1965)* suggested that a shallowly buried ribbon should be at least 20 times longer than it is wide to be considered as a legitimate two-dimensional object *(Blakely 1995 p. 191)*.

The most commonly used 2D model approach in gravimetry is to represent the model bodies with the two-dimensional objects with a polygonal cross-section extended to infinity on both sides perpendicularly to the profile. *Talvani et al. (1959)* derived a formula for computation of the gravitational effect g of the two-dimensional body with polygonal cross-section in the origin (x=0, y=0, z=0):

$$g = 2\,\gamma\,\rho\,\sum_{n=1}^{N} \frac{\beta_n}{1+\alpha_n}\left[\log\frac{r_{n+1}}{r_n} - \alpha_n\left(\tan^{-1}\frac{z_{n+1}}{x_{n+1}} - \tan^{-1}\frac{z_n}{x_n}\right)\right] \qquad (2.23)$$

where $\alpha_n = \frac{x_{n+1} - x_n}{z_{n+1} - z_n}$ and $\beta_n = x_n - \alpha_n\, z_n$.

This formula is often used in software packages providing two-dimensional gravity modeling *(Geosoft 2013; Saltus and Blakely 1993)* etc.

Two-dimensional profile modeling was widely used in case study examples in this Dissertation in a microgravity project *(Mantlík et al. 2009)* and medium-scale projects *(Mantlík and Karous 2013)*.

2.3.3 3D gravity models

As described in the introduction to this chapter, full three-dimensional modeling of the potential field has many limitations caused by problems with the constraining of data. Although production stage packages for 3D gravity modeling exist *(e.g. Geosoft 2013b)*, they suffer from both huge simplification of primary assumptions as well as complexity of model parameters. Nevertheless, methods extending 2D modeling by addition of a simple constrain in the third dimension can help in situations where a 2D model cannot represent the real situation precisely enough and where the full complexity of the 3D model is not necessary.

One of the possible approaches of simplification of the 3D situation is a method called 2¾D modeling, used in e.g. *Geosoft (2013)*. In this method, two-dimensional sources, as described in a previous chapter, are limited on both sides being extended beyond the limit using objects with the same polygonal cross-section and of different density. Thus, each anomalous object is described by it's density ρ, polynomial cross-section nodes coordinates x_i and z_i, limiting coordinates y_1 and y_2 and two densities ρ_+ and ρ_-, corresponding to the infinite parts of the body beyond the limits y_1 resp. y_2. Such increase in the number of model parameters still remains manageable while the complexity of the modeled geological situation can increase significantly.

Cady (1980) published algebraic solution of the integral 2.22 for the 2¾D polynomial body:

$$g = \gamma\,\rho \sum_{i=1}^{N}\Big[T_i \log r_{i+1}^2 - S_i \log r_i^2 + 2\,K_i \tan^{-1}\frac{T_i}{K_i} - 2\,K_i \tan^{-1}\frac{S_i}{K_i} + S_i \log\Big(\big(y_1 + R_{1,i}\big)\big(y_2 + R_{2,i}\big)\Big) - T_i \log\Big(\big(y_1 + R_{1,i+1}\big)\big(y_2 + R_{2,i+1}\big)\Big) + \frac{y_1}{c_i}\log\left(\frac{c_i S_i + R_{1,i}}{c_i T_i + R_{1,i+1}}\right) + \frac{y_2}{c_i}\log\left(\frac{c_i S_i + R_{2,i}}{c_i T_i + R_{2,i+1}}\right) + K_i \tan^{-1}\left(\frac{a^2 + y_1^2 + y_1 R_{1,i+1}}{z_{0i} T_i}\right) + K_i \tan^{-1}\left(\frac{a^2 + y_2^2 + y_2 R_{2,i+1}}{z_{0i} S_i}\right) - K_i \tan^{-1}\left(\frac{a^2 + y_1^2 + y_1 R_{1,i+1}}{z_{0i} S_i}\right) - K_i \tan^{-1}\left(\frac{a^2 + y_2^2 + y_2 R_{2,i+1}}{z_{0i} T_i}\right)\Big] \tag{2.24}$$

where $R_{j,i} = \sqrt{x_i^2 + y_j^2 + z_i^2}$, $K_i = {}^{a_i}/_{c_i}$, $S_i = x_i + x_{0i}$, $T_i = x_{i+1} + x_{0i}$, $c_i = \sqrt{1 - \left(\frac{z_{i+1} - z_i}{x_{i+1} - x_i}\right)^2}$, $a_i = {}^{z_{oi}}/_{c_i}$, $z_{0i} = z_i - x_i\,\frac{z_{i+1} - z_i}{x_{i+1} - x_i}$, $x_{0i} = \frac{z_{i+1} - z_i}{x_{i+1} - x_i}\,\frac{z_{0i}}{c_i^2}$.

First four terms of the Equation 2.24 represent pure 2D solution expressed in similar terms in the Equation 2.23. Remaining terms represent corrections for the limitation of the body at y_1 and y_2 respectively. Corresponding terms equal to zero or sum to zero for the whole polygon if $y_1 \rightarrow -\infty$ or $y_2 \rightarrow \infty$. Thus, the Equation 2.24 can be used to compute gravitational effect of all three parts of the 2¾D object.

2¾D modeling described above was widely used in the case examples presented in this Dissertation. In Appendix B *(Mantlík 2013)* the 2¾D model was used to estimate the gravitational effect of the railway rift and tunnel portal in order to introduce terrain corrections for this artificial structure. The results of such a model can be expected to fit the real field perfectly while a 2D model only would not provide satisfactory results.

In the case study of the complex structure of a sedimentary basin presented in Appendix C *(Mantlík and Matias 2010)*, two perpendicular series of 2D profile models were established. At the next stage, neighbor profiles were used to constrain properties of the environment on both sides of the profile and models were switched to 2¾D models. Finally, the models in both directions, N-S and E-W were compared and updated in order to make the crossings of profiles as identical in both directions as possible. As a result, the fully constrained model of the basin bottom was established in a grid which was as close to the full-featured 3D model as possible.

2.4 Interpretation of tectonic structure features

Equipped with the gravity modeling tools described in the previous chapter, the final stage of the project lifecycle takes place, establishing the interpretation model based on survey results. At this stage, reasonable geological meaning is assigned to each geophysical block delineated by the model. In addition to explanation of the physical properties of the delineated blocks in terms of their position in the geological model, description of identified linear structures is another important task during the interpretation stage.

Especially, in case of environmental projects, similar to the case studies presented in the appendices of this Dissertation, delineation of linear structures which are possible indicators of fault fracture zones are of great importance among others because of the principle importance of these structures in the hydrological cycle of the area under study.

Localization of tectonic zones in geophysical data can be a complicated task. Depending on the geological setting of the survey area, a tectonic structure itself can under some circumstances provide none or very weak contrast in physical properties detectable by geophysical methods. In such a situation, secondary effects caused by the development of the structure can be helpful, e.g. lateral change in physical properties of blocks on both sides of the fault zone. In addition, while the zone cannot be detected by one geophysical method, another method can possibly provide a reasonable signal. Interpretation of a complex of methods is highly desirable in such situations.

2.4.1 Gravity field tectonic structures indicators

Gravity indicators of the tectonic structures can be summarized as follows:

- Lateral density change

The most common indication of the tectonic structure is the presence of a strong interface in density distribution. Such a phenomenon is presented by a linear structure characterized by maximum value of the gradient of the gravitational field.

Transformations of the gravity field can be used to emphasize high gradient values. If the expected direction of structures is known, the directional derivative in the direction perpendicular to the expected structures can give the best results. If the direction is not known, total horizontal gradient and vertical derivatives of the field are the most useful transformations.

Methods for automatic picking of the linear structures based on searching for zones with maximum gradient of the gravity field were developed, e.g. *Blakely and Simpson (1986)*.

In the case study presented in Appendix C (Mantlík and Matias 2010) both methods were combined together to delineate structures in a preferred direction as well as secondary tectonic structures.

- Change of density in the fault zone

Process of development of the fault zone itself can cause physical properties changes in the fault zone. Fracturing and mechanical destruction of the material can cause increase of porosity and decrease of density of the fault zone material especially in its uppermost part *(e.g. Rao and Prakash 1990)*. Thus, the fault zone can be identified as a long-running negative anomaly at the fault position. In most cases, the effect of density decrease is weak and corresponding gravity anomaly does not significantly exceed the noise level. Correlation with other non-gravity methods is needed in such situations.

Density decrease indicator of tectonic zones in combination with other methods was used in the case study presented in Appendix B *(Mantlík and Karous 2013)*.

- No indication

Finally, a tectonic zone can be accompanied by no significant gravity signal. This fact should be taken into account when complex geophysical data are interpreted. Several examples presented in the Appendix B *(Mantlík and Karous 2013)* show strong fault zones indicators identified by e.g. resistivity profiling or seismic reflection while gravity did not provide any reasonable anomaly.

In similar situations, thorough assessment of the geological setting and available data has to be made in order to provide a final decision concerning possible fault location.

2.4.2 Non-gravity indicators

As mentioned above, gravimetry cannot be considered a reliable indicator of possible tectonic structures and combination with other geophysical methods is needed. The following list provides a brief overview of usability of other geophysical methods commonly used to indicate tectonics in combined projects.

- Geoelectric methods

The fact of the increase of porosity of rock material in the fault zone makes the electric resistivity methods first-choice option for searching for tectonic zones if ground water is present in the shallow layer.

Combination of gravity with resistivity profiling was successfully used for tectonic structures indication in the case study projects presented in Appendix B *(Mantlík and Karous 2013)*.

- Geomagnetic methods

Depending on local lithology, magnetometry can serve as a suitable counterpart method with gravimetry not only for fault detection, but for localization of lithological block boundaries in general. The necessary condition is, of course, contrast in magnetic properties (magnetic susceptibility) of structural blocks on both sides of the fault. Because of the low cost of the magnetic survey comparing to gravity, accompanying gravity with magnetics is reasonable in many situations.

Distinguishing litological blocks with similar densities from magnetic data was used in the case study example presented in Appendix B *(Mantlík and Karous 2013)*.

- Seismic methods

Change in mechanical properties of rocks inside the fault zones due to fracture development processes can be identified in seismic cross sections. In addition to change in the waveform picture, significant decrease of seismic wave velocity can be achieved at fault zones. Seismic reflection and refraction method was used as a secondary indicator for interpretation of geophysical profiles in the case study examples presented in Appendix B *(Mantlík and Karous 2013)*.

2.5 Use of interpreted gravity models in environmental studies

Being based not only on information concerning the interpretation of gravity data, but incorporating additional geophysical and geological constraining information, a typical interpreted gravity model provides a means for presentation of the point of view of the interpreting geo-scientist. In the process of construction of the gravity model, ambiguities of the solution are resolved based on additional independent data and the best result is selected from an infinite number of possible solutions. Geological and geophysical relevance of the model is the most important criterion in the process.

Common tasks in environmental studies which can be solved by integration of gravimetry with other geophysical methods are among others:

- Mapping and monitoring of closed landfills, industrial zones and other potential sources of pollution;
- Localization and monitoring of natural cavities, caves and undermined areas;
- Mapping and monitoring of the water table level, water reservoirs and hydrological structures including ground water temporal changes;
- Environmental projects needing deep vertical reach, e.g. geothermal studies;
- Regional structural studies, e.g. exploitation of large sedimentary basins.

Case study examples demonstrating complex interpretation of geophysical data in resulting interpreted gravity models are presented in the next chapter.

3 Interpretation of gravity data case studies

Three case studies of using gravimetry in complex of other geophysical methods for environmental problems and tectonic structure assessment are presented. Full texts of the articles presenting the case examples are attached as Appendix A – C of the Dissertation.

This chapter summarizes shortly the main topics covered by the case studies focusing on the problems directly related to the Dissertation theme.

3.1 Low-scale example: Landfill structure study, Ilhavo, Portugal

The low-scale example of a landfill structure study is presented in *Mantlík et al. (2009)*, Appendix A. of this Dissertion.

Landfills, especially those sealed in the past without prior detailed logs, pose, because of their complexity and heterogeneity, a challenging problem to geophysics. Micro-gravity prospection over a landfill extent can provide information about landfill shape because waste density can differ from the surrounding media density. Furthermore, internal zoning of the waste deposits can be investigated based on density changes inside the landfill.

Lateral and vertical boundaries of landfills were investigated e.g. by *Roberts et al (1990)* or *Silva et al. (2008)*. The difference in the presented case study is the very low contrast between the waste deposits and surrounding sediments. In addition, because of the setting of the landfill in the sand deposits, the density of local geological formations is expected to be low. It is the opposite of gravity to landfill characterization found in the bibliography. Thus, owing to the known heterogeneity of waste, one would expect to find both blocks showing density values greater and other blocks of lower density in comparison with the geological background.

The Ilhavo landfill presented in this study received mainly municipal deposits; nevertheless construction materials as well as metal are known to have been deposited as well. The landfill was sealed in 1999. Later the landfill was investigated by other geophysical methods *(Matias and Hermozilha 2006, Martinho and Almeida 2006)*.

The gravity survey at the Ilhavo landfill took place in January 2008. It was designed to study methodological aspects of the use of gravimetry in the landfill structure investigation in the area with low density contrast between the landfill material and surrounding media.

Two gravity profiles were established, the profile P1 was crossing the central part of the landfill and the parallel profile P2 was running approx. 400 m to the East. The main objective of profile P2 was to investigate the behavior of the regional gravity field in the vicinity of the landfill and to extract the regional component from the signal of the Profile P1.

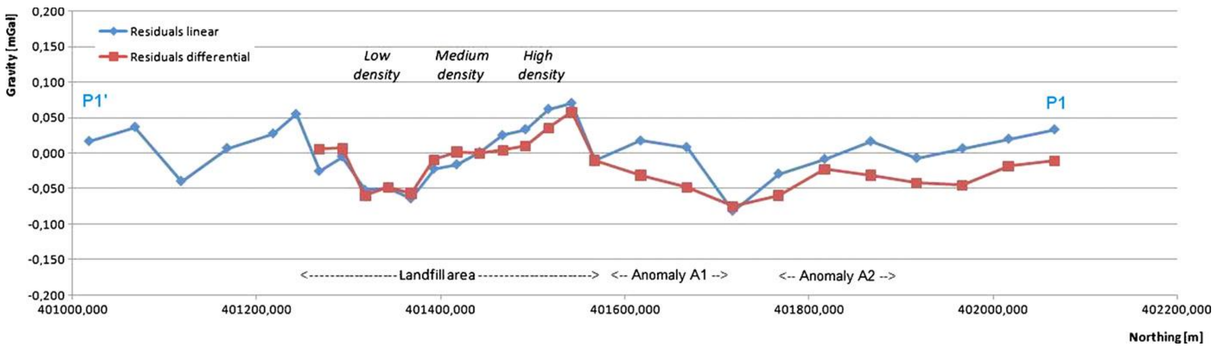

Figure 3.1: Residual gravity anomalies over the Profile P1. Blue line – linear fitting; red line – subtraction of the profile P2 data.

Two methods were used to establish and clear the regional field from the gravity data, standard linear polynomial fitting method and differential method, i.e. method based on regional field shape fitted from the Profile P2. *Figure 3.1* presents a residual gravity field at Profile P1 after regional field established with the use of both methods was extracted. Figure 3.1 shows that influence of both small anomalies A1 and A2 noticed at Profile P1 out of the landfill extent are significantly lowered for the differential method regional field removal. At the landfill extent, the difference is not as pronounced, but still significant.

Gravity survey was accompanied with the detailed differential GPS (DGPS) topographic survey with precision better than 2 cm serving for both reductions of gravity data and the computation of local terrain corrections.

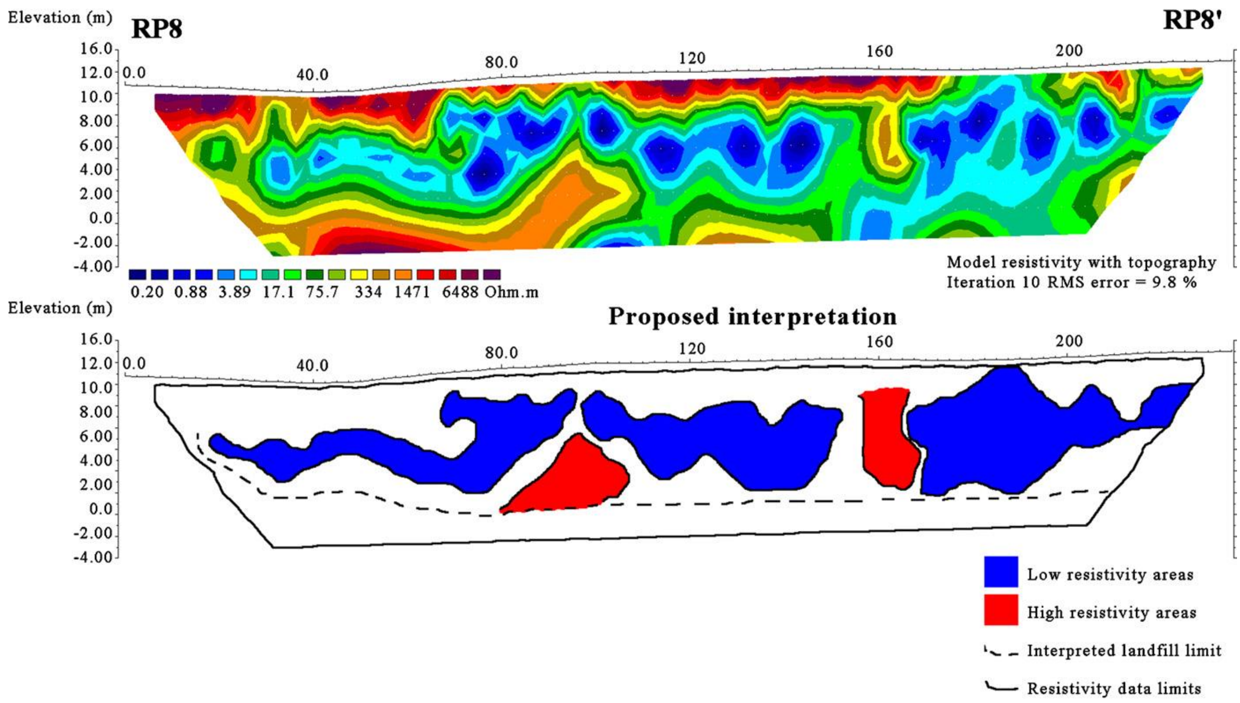

Figure 3.2: The resistivity profile RP8.

In addition to the gravity survey, resistivity survey in three profiles running over the landfill extent was made. Wenner-Schlumberger array scanning took place and obtained apparent resistivity distribution was inverted with the use of RES2Dinv software *(Geotomo 2013)*. Results of the resistivity inversion were used as constraining information for gravity data models. Figure 3.2 shows resistivity inversion results for the Profile RP8 running approx. parallel to Profile P1.

Finally, taking into account constrains given by resistivity data, a simple gravity model of the landfill structure was established as presented at *Figure 3.3*. As the vertical extent of the landfill material was given by results of the resistivity survey, lateral changes in density can be estimated based on gravity data as shown on the model.

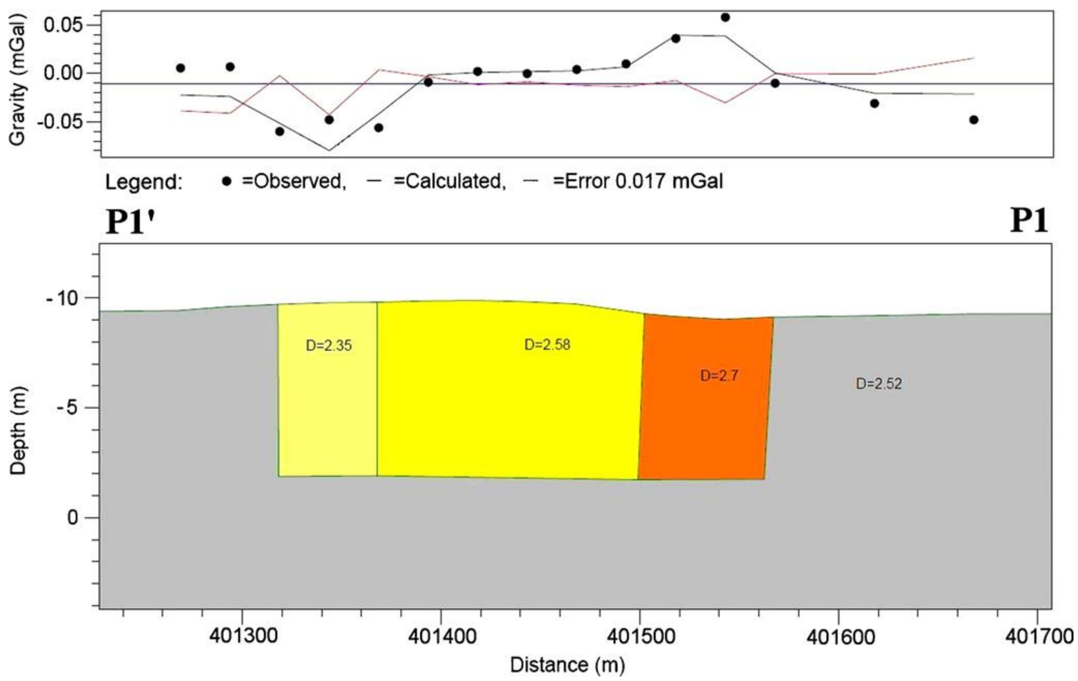

Figure 3.3: Gravity model of the Ilhavo landfill. The depth of the landfill deposits was determined from the resistivity data interpretation that allowed estimating the overall densities differences between the three zones inside the landfill.

The presented case example shows the possibility of determining the internal structure of the landfill even when it is located in the low-density sedimentary formations. The gravity modeling was only possible using the additional resistivity and borehole information to reduce ambiguity in the potential field modeling.

As there are no logs describing the materials and internal composition of the landfill under study, the presented case study shows that geophysics can play an important role in the internal characterization of a landfill. Hence, any future drilling operations, for economic development or monitoring purposes, can take important advantage of the model proposed.

3.2 Medium-scale examples: Hydrothermal energy exploitation areas in the CR

Three areas of possible hydrothermal energy exploitation in the CR were surveyed by a complex of geophysical methods. The construction of gravity interpretation models based on the interpreted data is presented in the case study. A full text of the article can be found in Appendix C.

Interest in geothermal energy exploitation has grown in the last few years because of increasing fossil fuel prices. Pilot projects using geothermal energy for electric energy production by the Hot Dry Rock method are under consideration in the Czech Republic *(Myslil (ed.) 2011)*.

Geophysical prospection at future prosperous geothermal exploitation site should focus on the following tasks:

- Determine the thickness and structure of sedimentary cover
- Delineate the extent and boundaries of geological/geophysical units with a vertical reach of at least 500 to 2000 m
- Map tectonic structures, especially deep penetrating fault zones

Detailed knowledge of local geology, physical properties of rocks and tectonics of the future exploitation area is needed to select proper locations for the production geothermal drills. A properly selected suite of surface geophysical methods can provide an efficient way of obtaining the required information using a reasonable amount of resources *(Kelly et al. 1993)*.

Gravity modeling constrained by geological knowledge about the survey area and results of interpretation of other geophysical methods was selected in the presented case study areas.

Seismic reflection data in combination with the interpretation of vertical electric sounding data were used to determine the vertical scale for the gravity profiles. In addition, seismic refraction was helpful in determining the thickness of the low velocity / low density nearsurface sediments. Profile resistivity was used to determine the presence of conductive zones possibly indicating faults and other tectonic structures as well as the lateral extent of individual geological units. Profile magnetometry data added more information on the physical properties of individual blocks.

Three areas were selected as case studies, locality Nová Paka, Lovosice and Frýdlant in the Czech Republic.

The **Nová Paka** locality *(Figure 3.4a)* is located on the edge of the “Krkonošská pánev” Permo-Carbonian basin. The basin is partially covered by sub-horizontal layers of Cretaceous sediments penetrated by several neo-volcanic bodies. The expected dominant tectonic structures are oriented E-W, secondary orientations are NW-SE resp. N-S *(Karous and Myslil 2009 pp. 12-13; Chaloupský 1998)*.

An area of about 1 km^2 was surveyed by five geophysical profiles perpendicular to expected orientations of the tectonic structures *(Figure 3.4a)*.

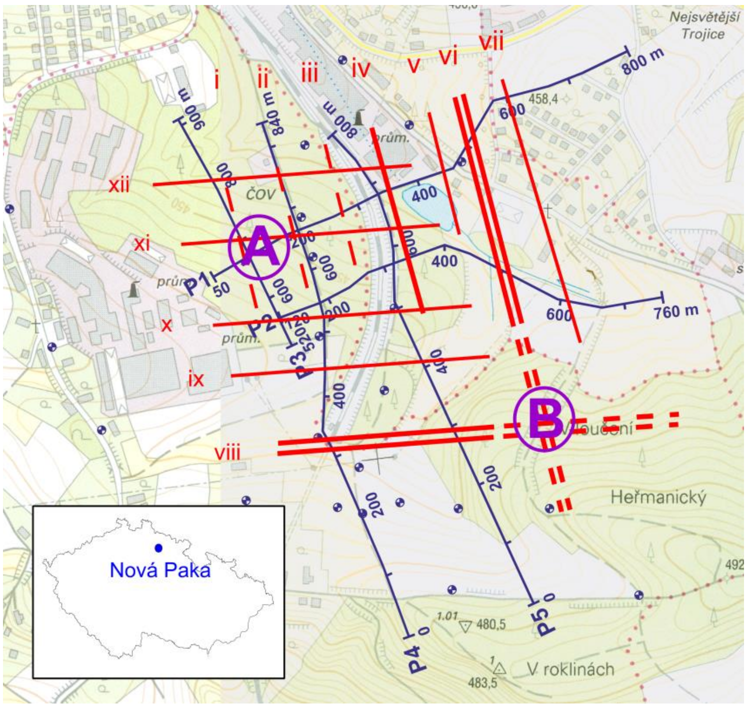

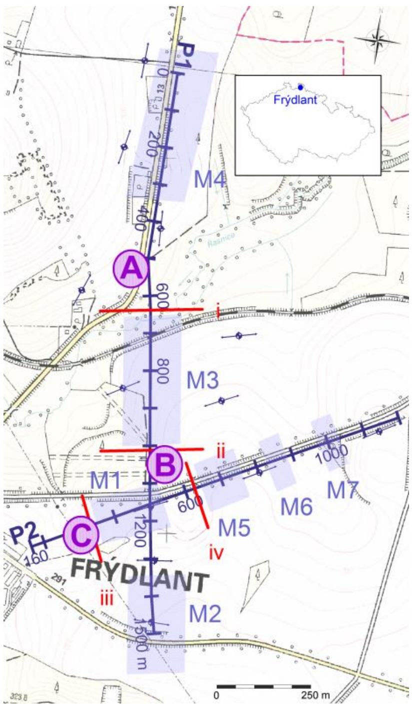

a) Nová Paka *c) Frýdlant*

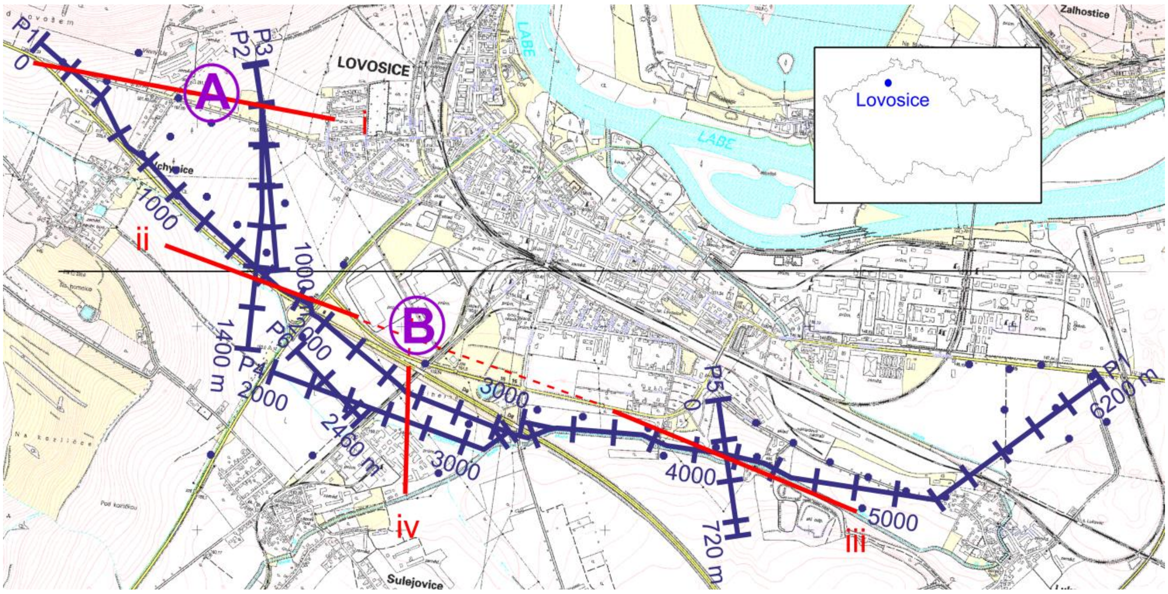

b) Lovosice

Figure 3.4: Situation of case study areas with geophysical profiles and VES sites (blue lines and blue spots), interpreted tectonic structures (red lines) and prospective zones for further exploitation (magenta capital letters).

The main geological unit in the **Lovosice** area *(Figure 3.4b)* is crystalline basement covered by Permo-Carbonian and High Cretaceous sediments. The total thickness of the sedimentary formations in the area of interest reaches 1000 m. Several granitoid bodies appear in the crystalline complex with a possibly relatively high concentration of radioactive materials.

Expected main orientations of tectonic structures are Litoměřice fault zone orientation, i.e. approx. E-W or NW-SE, and secondary N-S orientation *(Karous 2007)*. Six geophysical profiles were laid out in the Lovosice survey area.

The area of interest in the **Frýdlant** locality, 2 x 1 km in size, belongs to the "Krkonošsko-Jizerské krystalinikum" crystalline complex. It is penetrated by tertiary basalt volcanic bodies and covered by quarternary glacio-fluvial sediments *(Kozdrój et al. 2001; Karous and Myslil 2007)*.

Two nearly perpendicular geophysical profiles were established in the Frýdlant area *(Figure 3.4c)*.

In addition to the gravity data acquisition, resistivity profiling, vertical electric sounding, profile magnetometry, seismic reflection and refraction survey took place along the selected geophysical profiles. Details concerning data acquisition parameters and processing procedures for individual methods can be found in *Appendix C*.

Equipped with processed and interpreted data from each geophysical prospection method, an integrated interpretation and modeling stage, based on comparing and contrasting individual results, was employed. A detailed model of the area was constructed using the best possible conformity with the available data.

Two-dimensional interpretation gravity models were constructed for all profiles where gravity data were collected. All available data from other methods were used as constraining information. This included delineation of individual geophysical blocks including possible tectonic structures, estimates of thicknesses of individual layers, information about rock densities based on older drilling data and regional gravity models etc. *(Karous 2007; Karous and Myslil 2007; Karous and Myslil 2009)*.

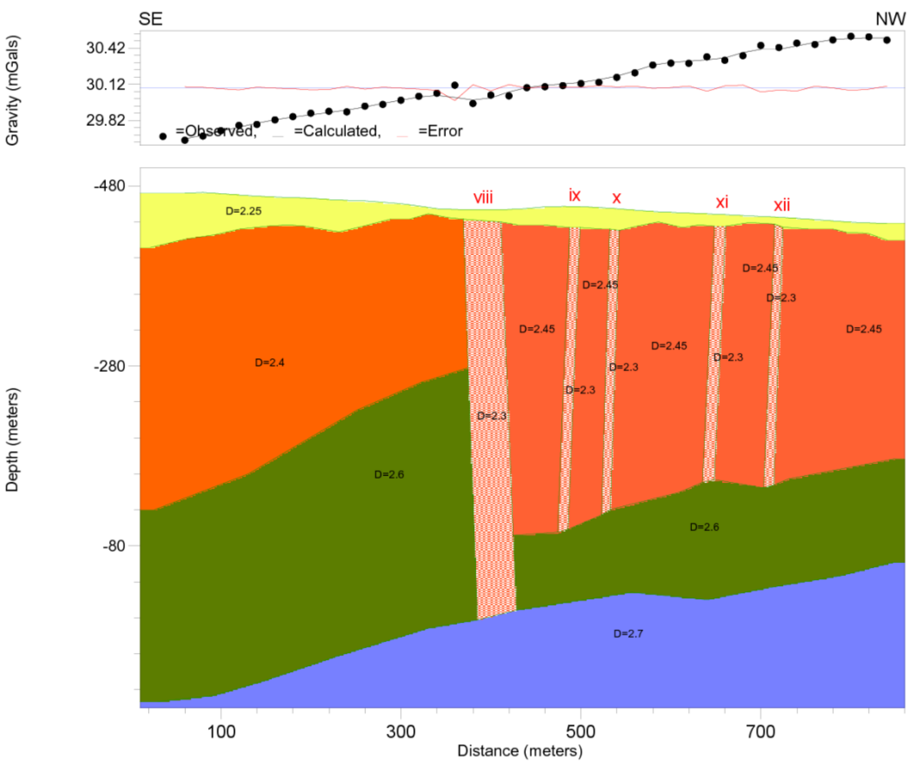

Figure 3.5a. Profile P4 at the Nová Paka locality

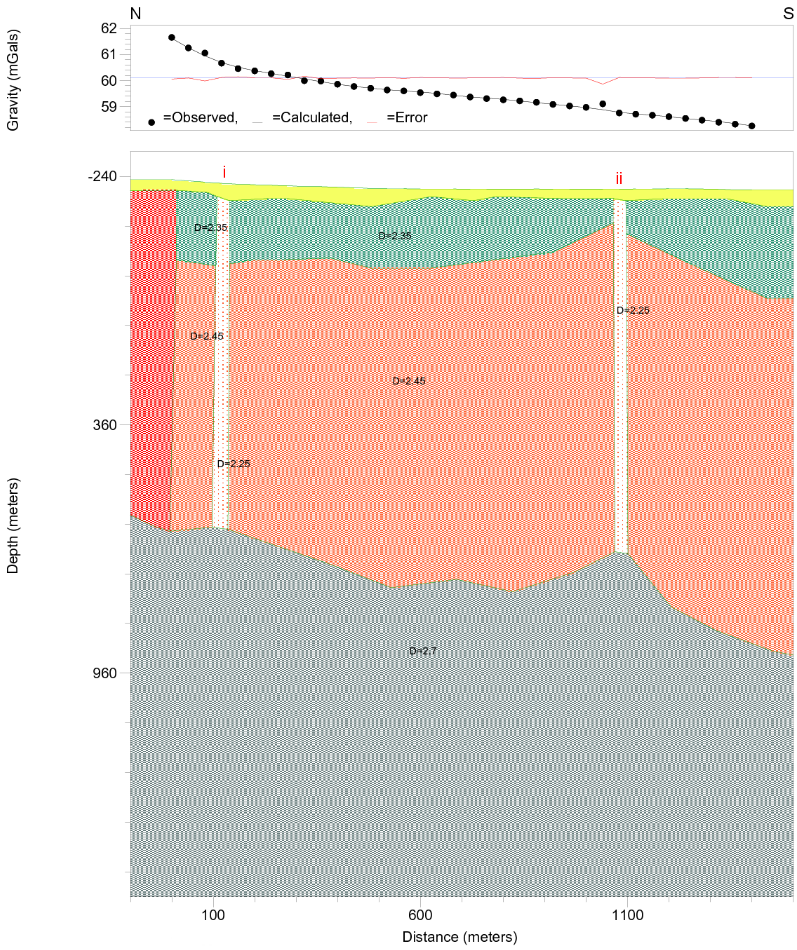

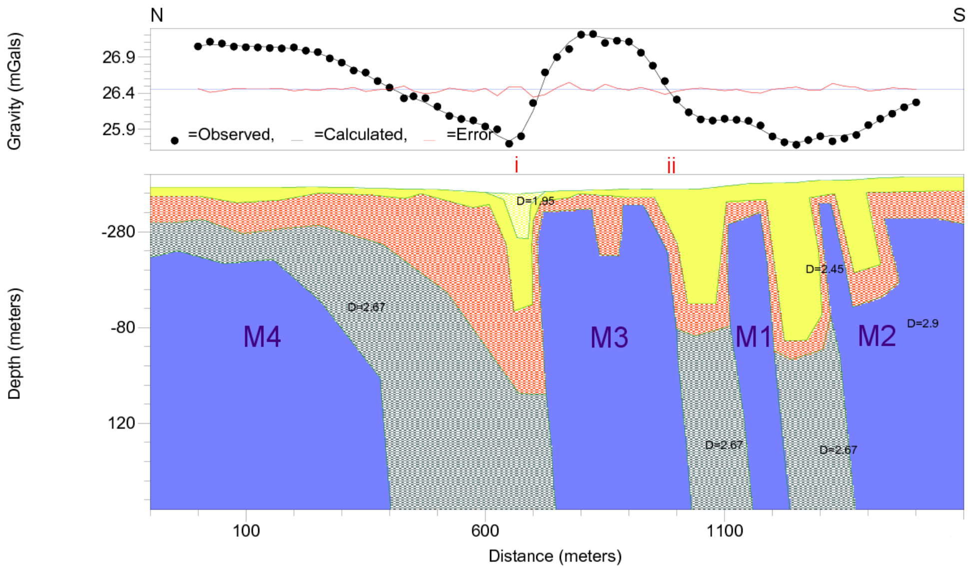

Figure 3.5. b) (upper) Profile P2 at the Lovosice locality, c) (lower) Profile P1 at Frýdlant.

Examples of the interpreted gravity models are presented at *Figure 3.5 a) - c)*.

Based on interpretation of the gravity models, prospective zones of interest for further exploration were delineated for each area.

Two prospective zones expected to behave as possible thermal heat corridors were interpreted at the Nová Paka locality. They are located at the projected intersections of tectonic zones interpreted from profile data. Similarly two zones were delineated in the Lovosice locality. Finally, three zones of interest were determined at the Frýdlant locality.

Although most structures interpreted and presented in the gravity models are accompanied by a significant gravity signal, some tectonic features, clearly detected by other methods, do not provide a significant gravity response. Thus, thorough selection of the set of the geophysical methods based on an assessment of expected physical properties of rocks and tectonic structure of the area under study is very important.

The presented case study examples show that interpretation of detailed profile gravimetry data can be effectively supported by data obtained in a framework of properly selected geophysical methods. The latter can serve as an important source of constraining information especially in the complex geological setting encountered in geothermal applications. It follows that two-dimensional geophysical survey can effectively be used to reduce exploration costs in geothermal projects.

3.3 Regional-scale example: Sedimentary basin basement tectonic structures assessment in Aveiro Basin, Portugal

The regional-scale case example presenting the basin structure study was published in *Mantlík and Matias (2010)*. A full text of the article is presented in Appendix B. of the Dissertation.

The Aveiro basin in Northwest Portugal is a coastal region characterized by gentle topography and lowlands. Thus, it has a high degree of vulnerability to sea level changes. The Atlantic Ocean load on the coastal regions of the basin has been increasing steadily. It causes evident side effects on land development and management as well as ground water resources and exploitation. Understanding the internal structure of the basin is therefore very important, especially when focused on groundwater resources, strategic decisions on land development and the investigation of offshore structures and potentialities.

Bearing in mind the geological, geographical and geomorphological conditions of the basin, the gravity method is well suited to providing geological and tectonic information of the region.

The gravity survey consisting of 653 stations covering the area of the basin with average density of four readings per km^2 took place in 2001 *(Figueiredo 2001)*. In that work all available geological and geophysical information was integrated but only limited two-dimensional gravity models were made. The models presented in *Figueiredo (2001)* were used as a starting point for this more detailed work.

From the geological point of view, the Aveiro basin, locally called “Ria de Aveiro”, is the most northerly part of the Portuguese Western Mesosoic Margin, called “Lusitana Basin” *(Silva and Andrade 1998)*. It is a sedimentary basin adjacent to the Hesperian massif, craton border type with low subsidence where sedimentation occurred over the continental crust. The Precambrian basement is located in absolute heights ranging from -200 to -500 m in the coastal zone. The basin is affected by the strike-slip faulting *(Mougenod et al. 1986)*.

The succession of deposits over the Precambrian basement includes Triassic sandstones and Medium to High Cretaceous deposits, covered in places by old beaches and fluvial Pleistocene deposits. In the coastal zone, these deposits are covered by recent Holocene sediments.

Two major fracture systems have been recorded, striking north-south and NNW-SSE. The N-S system represents the reactivation of Variscan strike-slip faults, a further NNW-SSE system could be related to the late Hercynian deformations *(Silva and Andrade 1998)*.

The sedimentary formations of the basin show little deformation, however post Hercynian movements caused fractures in the basement and horsts and grabens were produced. As a result, various blocks of individual shape and development were created *(Barbosa 1981; Casas et al. 1995; Teixeira and Zbyszewski 1976)*.

The basin generally plunges to the southwest reaching depths greater than 400 m in its deepest part. Because the major density contrast is expected between the sedimentary cover and the basement, the depth of the basement can mainly be investigated and modeled from gravity data.

For processing in this case example, gravity data from an earlier survey *(Figueiredo 2001)* were considered. Two methods were applied to separate regional field from the data, a plane regional field model and a third-order surface regional field model. *Figure 3.6* presents contour maps of the initial complete Bouguer anomaly field and residual gravity field after separating the regional field from the data with the use of both methods.

In general, the Bouguer anomaly in *Figure 3.6a* shows the overall shape of the basin with the most pronounced structures. To the NE higher values are revealed and the basin bottom must therefore be closer to the surface in this area while the lowest values corresponding to the deepest parts of the basin in this region are depicted to the SW.

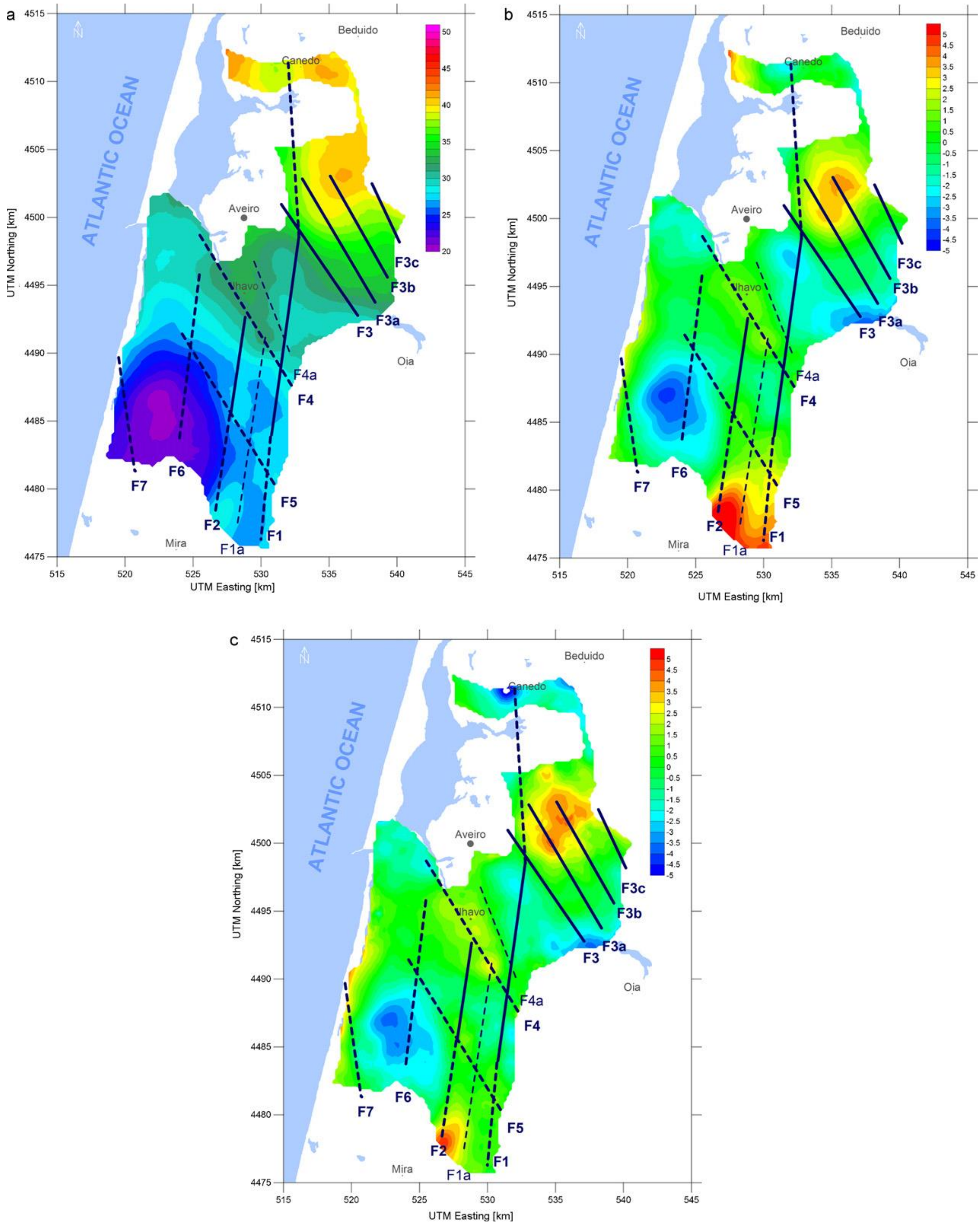

Figure 3.6: a) Bouguer anomaly map, b) residual field after removal of linear trend, c) residual field after removal of the regional field modeled by the 3rd order surface. Units are mGal.

The maps in *Figure 3.6b and 3.6c* corresponding to the residual field provide a clearer picture of local structures while the overall basin shape and the most pronounced anomalies disappear as expected. Thus, the analysis of the gravity field after regional model removal is suitable for the determination of local tectonic features at the bottom of the basin.

As the next step, horizontal gradients of the anomalous field were computed, particularly the horizontal gradient in NS direction and EW direction as defined by *Equations 2.15 and 2.14*.

Because of strong directional dependence of the horizontal gradients and with respect to the expected main strike directions of the tectonic structures, the E-W gradient should provide extreme values at the N-S oriented structures. On the other hand, E-W structures would be most pronounced at the N-S gradient map. Unfortunately, the secondary structures direction, NNW-SSE does not follow either of the computed gradients directions, hence only the N-S structures can be expected to be identified clearly in the horizontal gradient maps. Correlation with other systems will be less pronounced.

Figure 3.7 presents horizontal gradient maps together with a map of the second vertical derivative field. The last is not directional-dependent and as such provides information independent from the direction of structures. On the other hand, a significant level of noise is present in the second vertical derivative map compared to the horizontal gradients.

In addition to the gradient maps, downward continuation maps of the gravity field were calculated. Downward continuation moves the field measured at the planar surface closer to the sources of the field, in the case of the Aveiro basin closer to the basin bottom structures. Downward continuation is defined by *Formula 2.21*. The procedure behaves as a high-pass filter. As such, high frequency noise is amplified by the transformation in favor of the useful signal. This fact limits usefulness of the downward continuation.

For illustration, *Figure 3.8* presents horizontal gradients similar to the gradients presented in the Figure 3.7, but computed from the 200 m downward continued gravity field.

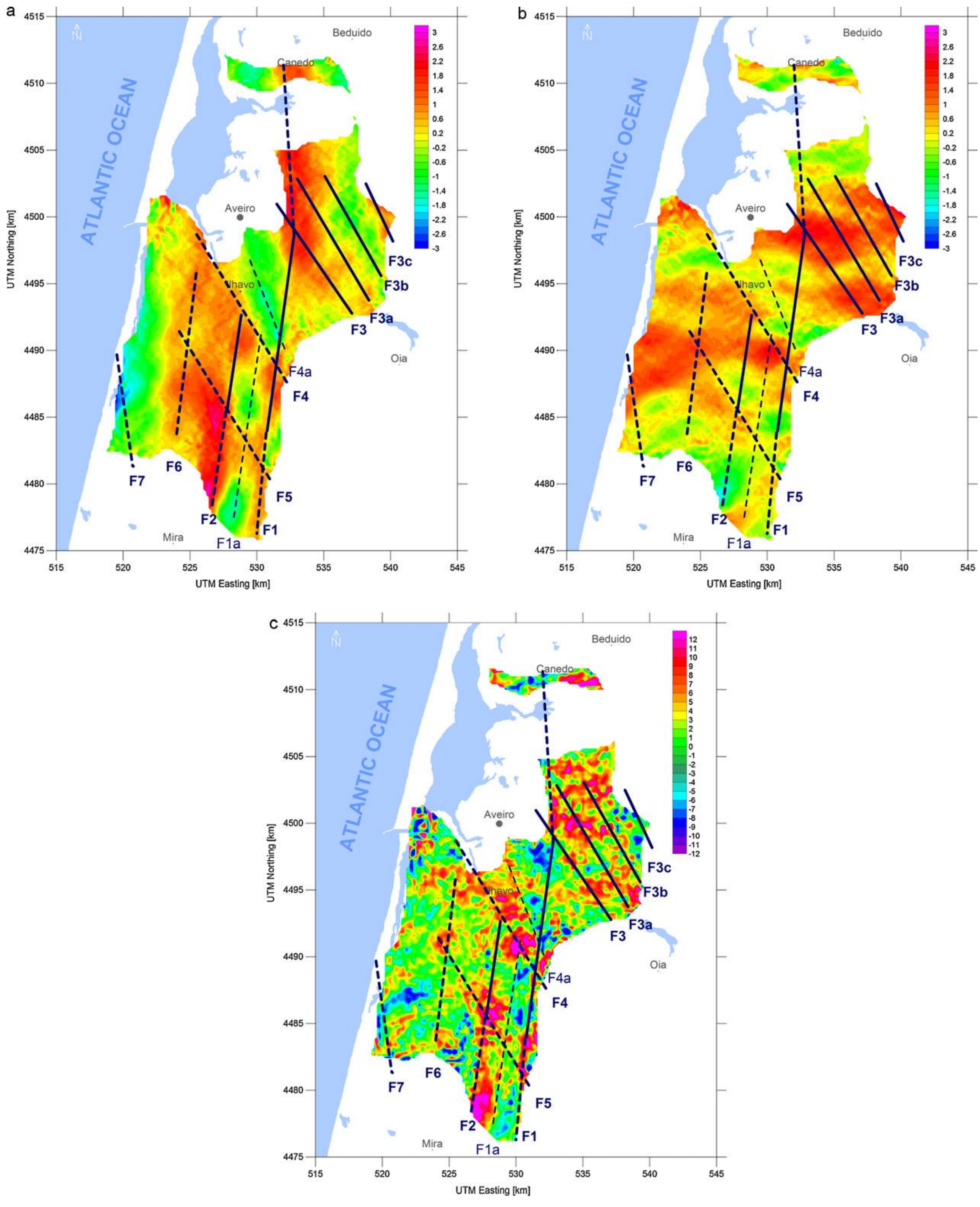

Figure 3.7: a) E-W horizontal gradient map, b) N-S horizontal gradient map, c) second vertical derivative map. Units are mGal/km resp. mGal/km^2.

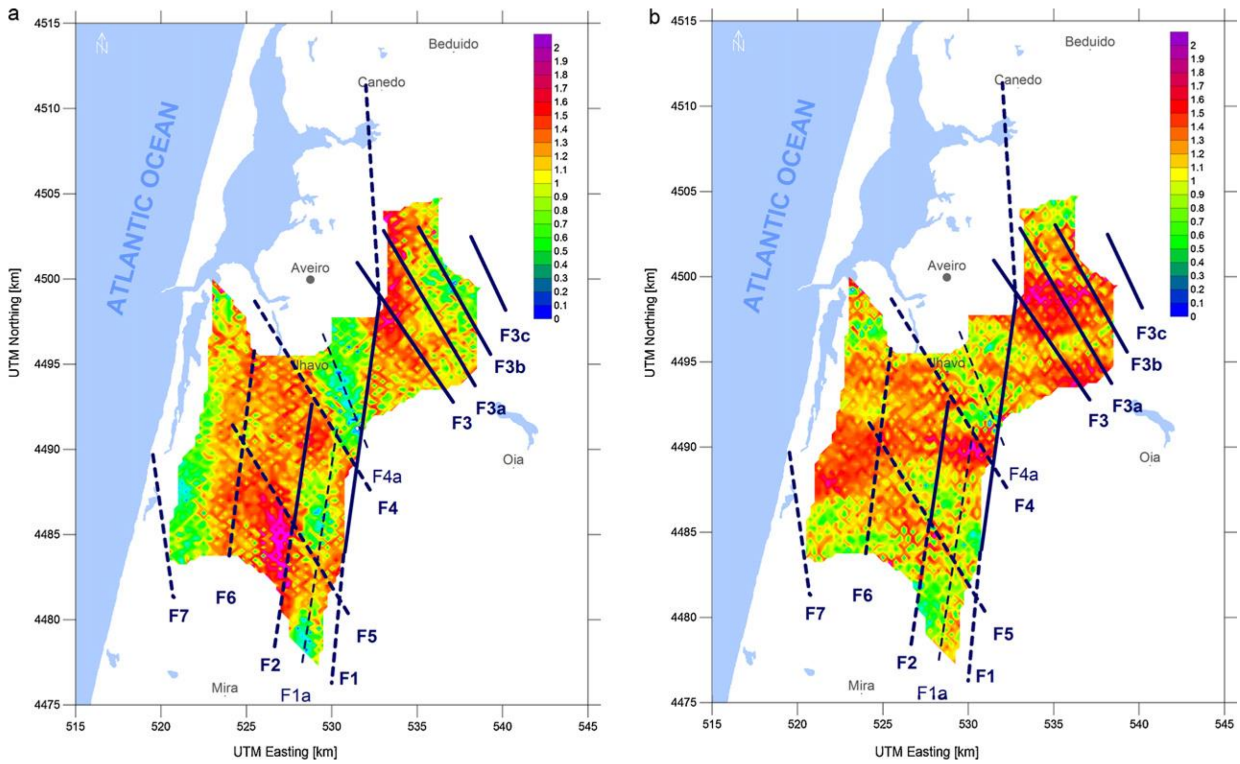

Figure 3.8: Horizontal gradients computed from the 200 m downward continued gravity field of the Aveiro basin a) E-W direction, b) N-S direction.

Regardless of the significant increase of short-wavelength noise, the gradients computed from the downward continued field show in some aspects a sharper signal than the gradients computed from the original field presented in *Figure 3.7*.

Based on the data processing described above, two detailed gravity models were constructed:

- The model based on the complete Bouguer anomaly field presenting the overall shape of the basin and the major structures. The depth of sedimentary coverage of the basin was constrained by available geological and geophysical data *(Figueiredo 2001)*, i.e. drill logs and geological profiles interpreted from deep resistivity sounding data;

- The model based on the residual gravity field. The overall shape of the basin is suppressed in this model but more pronounced details of the buried tectonic structures are visible.

Figures 3.9 a) and b) present Bouguer anomaly field models while Figures 3.9 c) and d) present residual field models. Maps a) and c) present E-W profiles and maps b) and d) present N-S profiles. Detailed description of procedures used for the creation of the presented models can be found in Appendix B.

The map of the basin bottom shape was plotted as a final step of the modeling *(Figure 3.10)*. The map was constructed as the depth of the interface between the Triassic sandstone and the Precambrian basement rock geophysical layers as interpreted from the models at Figure 3.9 a) and b) together with the interpretation of tectonic features.

The interpretation of tectonic features is based primarily on the gravity field analysis. Horizontal gradients and vertical derivatives were very useful at this stage of interpretation. Then the interpreted features were compared to the gravity models both using the Bouguer field and the residual field models. Based on the results, the gravity models have been constrained and, as necessary, interpreted tectonic features were repositioned to better fit the properties of the model.

The results represent the unique quantitative geophysical mass distribution models as derived from the comprehensive interpretation of the geological and geophysical data set of the basin. The data processing procedure was applied in the same manner over the whole area under investigation.

Parameters of the model were constrained by the data. Thus, the presented model is well established and homogenous over the whole area including parts without further reliable geological or geophysical information.

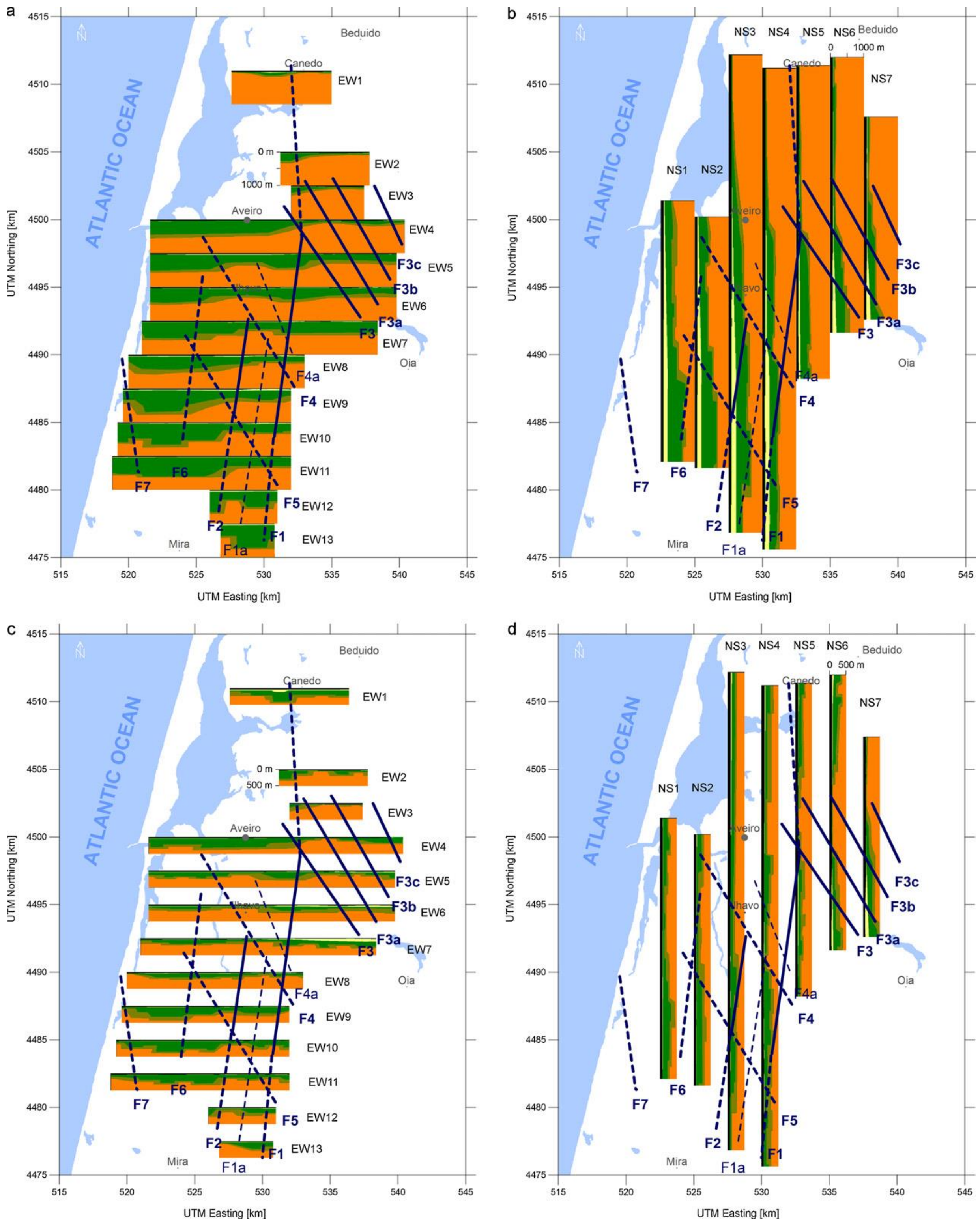

Figure 3.9: Density distribution models based on gravity field analysis. a) and b) Bouguer field model, c) and d) residual field model.

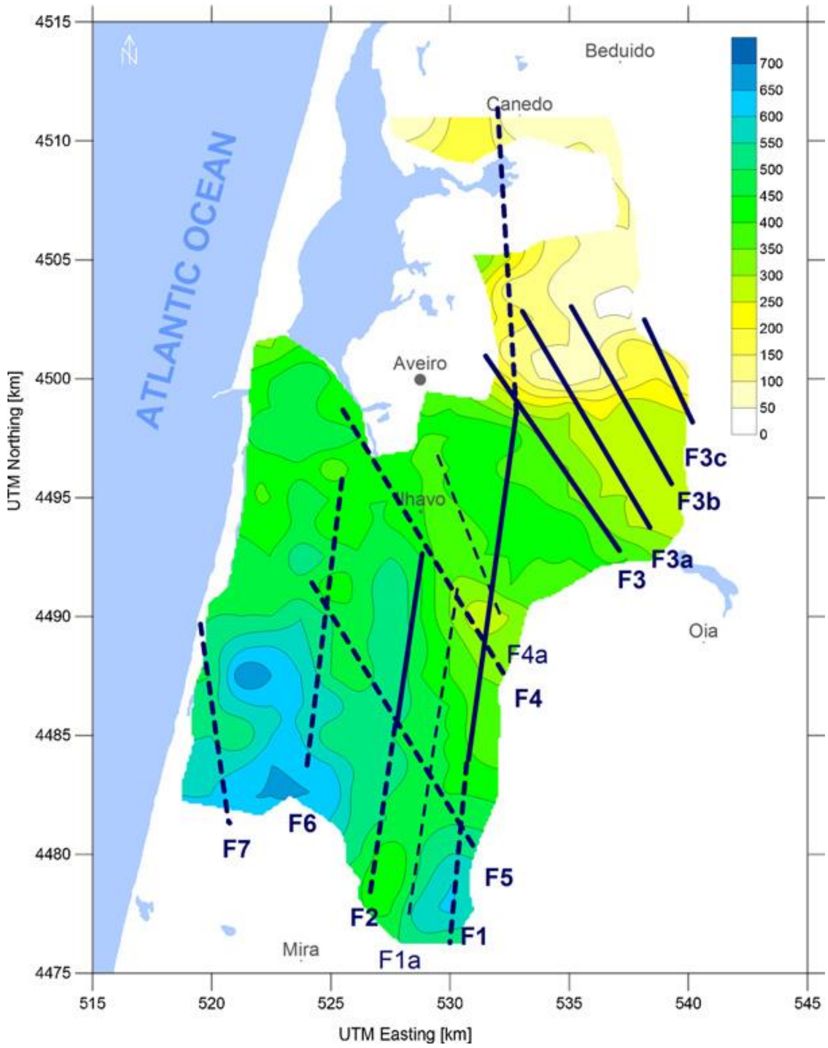

Figure 3.10: Map of the tectonic features interpreted from the gravity data analysis together with the basement depths from the Aveiro basin in meters as interpreted from the gravity model.

Detailed knowledge of the internal structure of the basin is of great importance for future investigation and exploration of the whole region. The results can be used as useful tools for future underground water exploration and exploitation as well as borehole location planning.

Bearing in mind the geomorphology of the basin, the gravity method proved to be an economical tool for investigating basin structures.

4 Conclusions

Three projects demonstrating current possibilities in the practical usage of interpreted gravimetry data in conjunction with further geophysical and geological information were presented.

In the first project, the internal structure of a sealed landfill was determined with the use of gravimetry in conjunction with other methods. Three blocks with different densities were delineated inside the landfill. Interpretation of the gravity anomalies was possible because of the existence of resistivity array scanning data which provided constraining information concerning the vertical extent of the landfill.

In the landfill project, another interesting innovative approach was used. The regional gravity signal was determined with the use of fitting data from a reference profile established out of the landfill area. Thanks to this procedure, the gravity signal over the landfill extent was cleared from the signal caused by deeper and larger structures.

The Ilhavo landfill is situated in the sand deposits with density very close to the densities of the deposited material. Thus, there was no significant contrast between the landfill deposits and the surroundings. The presented study shows that constraining gravity data by additional information, resistivity array scanning in this case, can work around this problem.

The medium scale case histories, presented in this work as the second project, present an approach used for delineation of deeper structural features in order to determine prospective zones for possible hydrothermal exploitation in selected areas. Two-dimensional gravity models were constructed with the help of constrains provided by a complex of geophysical methods as well as geological assumptions available.

Three areas with different geological settings were selected for the prospection. A complex of geophysical methods was acquired at selected profiles for every area. Processed data were interpreted and the results of interpretation were used for the construction of complex two-dimensional interpretation models. Based on modeling results, prospective zones for further investigation were established.

The presented case study provides interesting methodological material which demonstrates both advantages and disadvantages of all the used methods. In different geological settings it can be useful reference information for the selection of methods for future projects with similar goals. As an example the cross-coupling of gravity indications of fault zones and indicators provided by resistivity profiling where some structures were not identifiable by gravity data only while resistivity data provided clear anomaly and vice versa, can be presented.

Finally, the regional project focused on interpreting the detailed structure of a sedimentary basin was presented. In this case study, older regional data were re-interpreted in order to provide a detailed density distribution model.

In contrast to the other projects presented in this Dissertation, no survey based on other geophysical methods took place. Instead, the gravity model was constrained by geological, drilling and geophysical data available from older studies only. In addition, most such information was available for the northern part of the survey area only. Unified processing and interpretation procedure over the whole extent of the survey area allowed extrapolating results of gravity modeling from the well-established northern part of the basin to the South with a high level of reliability.

In addition to the comprehensive two-dimensional gravity modeling used in previous projects as well, transformations of the gravity field were used to determine delineations which can indicate possible tectonic structures buried below the basin sediments. The interpretation of linear structures from the transformed gravity field was proved to be in good correlation with results of the gravity models as well as with the geological situation.

It can be concluded that the projects presented in the Dissertation provide practical presentation of methodological approaches suitable for the resolution of a wide range of both environmental and tectonic structure problems.

5 References

Barbosa B.P. (1981): Geological map of Portugal, sheet 16-C, Vagos, scale 1:50000. Serv. Geol. Portugal, Lisboa [in Portuguese].

Blakely J. Richard (1995). Potential Theory in Gravity & Magnetic Applications. *Cambridge University Press. 0-521-57547-8.*

*Blakely, R. J. and Simpson, R. W. (1986): Approximating edges of source bodies from magnetic or gravity anomalies. Geophysics **51**, 7, 1494-1498.*

*Cady J. W. (1980): Calculation of gravity and magnetic anomalies of finite-length right polynomial prisms. Geophysics **45**, 10, 1507-1512.*

*Cartwright D. E. and Edden A. C. (1973): Corrected Tables of Tidal Harmonics. The geophysical journal **33**, 3.*

*Cartwright D. E. and Tayler j. R. (1971): New Computations of Tide Generating Potential. The geophysical journal **23**, 1.*

*Casas, A., Matias, M., Rivero, L., Silva, M., (1995): Preliminary Gravimetric study of the Aveiro lagoon. Geociencias. Univ. de Aveiro **9**, 23–33 [In Spanish].*

Chaloupský, J. (editor), 1998, Geologická mapa ČR 1 : 50 000, list 03-41 Semily (Geological Map of the CR 1 : 50 000, Sheet 03-41 Semily): Česká geologická služba (Czech Geological Survey). On-line version: http://www.geology.cz/app/ciselniky/lokalizace/index.php accessed 21 January 2013.

*Doodson A. T. (1954): The Harmonic Development of the Tide Generating Potential. Proceedings of the Royal Society. Series A100. 306-328. London, 1921. Reprint. International Hydrographic Revue **31**, 1.*

Elkins, T.A. (1951): The second derivative method of gravity interpretation. Geophysics 16, 29–50.

Figueiredo, F. (2001): Applied Gravity to the geometric organization of the Meso-Cenozoic formations – Baixo Vouga. Ph.D. thesis, Coimbra, Portugal, 213 p. [in Portuguese].

Geosoft (2010): Montaj Gravity & Terrain Correction, Gravity Data Processing Extension for Oasis Montaj v7.1 TUTORIAL and USER GUIDE. http://www.geosoft.com/resources/goto/gravity-and-terrain-correction-tutorial-english visited April 7, 2013.

Geosoft (2013): GM-SYS Profile modelling. http://www.geosoft.com/products/gm-sys/gm-sys-profile-modelling visited April 5, 2013.

Geosoft (2013b): GM-SYS 3D modelling. http://www.geosoft.com/products/gm-sys/gm-sys-3d-modelling visited April 5, 2013.

Geotomo Software (2013): Geoelectrical Imaging 2D & 3D. http://www.geotomosoft.com/products.php visited April 14, 2013.

Grant F. S. and West G. F. (1965): Interpretation theory in applied geophysics. McGraw-Hill.

Hammer S. (1939): Terrain corrections for gravimeter stations. Geophysics. ***4****, 3, 184-194.*

Jung K. (1953): Zur bestimmung der bodendichte nach dem Nettletton-verfahren. Zeit. für Geophysik, ***19*** *(Sonderband), 54-58.*

Karous M. (2007): Závěrečná zpráva geofyzikálního a geotermálního průzkumu okolí města Lovosice (Final report on geophysical and geothermal exploration of the surrounding of the city of Lovosice). Geomedia, Geonika and Ministry of Environment CR.

Karous M. and Myslil V. (2007): Doplňkový geotermální a geofyzikální průzkum území východně od Frýdlantu v Čechách (Complementary geothermal and geophysical exploration of the locality east of Frýdlant v Čechách). Geonika, Miligal and Ministry of Environment CR.

Karous M. and Myslil V. (2009): Geologické práce pro využití geotermální energie v oblasti Nové Paky. Závěrečná zpráva. (Geological exploration for exploitation of geothermal energy resources at the locality Nová Paka. Final report.). Geonika, Geoterm, Miligal and Ministry of Environment CR.

Kelly W. E. and Mareš S. (editors) (1993): Applied geophysics in hydrogeological and engineering practice. Elsevier.

Kozdrój, W., Krentz O. and Opletal M. (editors) (2001): Geological map and comments on the geological map Lausitz, Jizera, Karkonosze (without Cenozoic sediments) 1 : 100 000. Państwowy Instytut Geol.

Longman I. M. (1959): Formulas for computing the tidal accelerations due to the Moon and the Sun. *Journal of Geophysical Research **64**, 2351-2355.*

Mantlík F. (2013): BlueWhaleProcessing Geophysical Software – User's Guide. *http://bluewhaleprocessing.com/bwpupdates/installers/Documentation.pdf visited March 31, 2013.*

*Mantlík F., Matias M., Lourenco J., Grangeia C. and Tareco H. (2009): The use of gravity methods in the internal characterization of landfills – a case study. Journal of Geophysics and Engineering **6**, 357-364.*

Mantlik F. and Karous M. (2013): Use of gravimetry in detailed geophysical prospection of potential geothermal energy exploration areas: Case studies in the territory of the Czech Republic – submitted to Geophysics.

*Mantlik F. and Matias M. (2010): Interpretation and modelling of regional gravity data of the Aveiro Basin (Northwest Portugal). Comptes Rendus Geoscience, **342**, 823-836.*

*Martinho E. and Almeida F. (2006): 3D behaviour of contamination in landfill sites using 2D resistivity/IP imaging: case studies in Portugal. Environ. Geol. **49**, 1071–1078.*

Matias M. and Hermozilha H. (2006): A 3D Constant Offset GPR survey on Il´havo Landfill. Proc. of 12th European Meeting of Environmental and Engineering Geophysics (Helsinky, Finland A031), 5 pp.

Mougenod D., Kidd R.B., Mauffret A., Regbauld H., Rothwell R.G., Yvanney J.R. (1986): Geological interpretation of combined Seabeam, Gloria and Seismic data from Porto and Vigo Seamounts, Iberian continental margins. Mar. Geophys. Res. ***6****, 329–363.*

Myslil V. (editor) (2011): Geotermální energie: Zdroje, využití, technologie (Geothermal energy: Resources, Exploitation, Technologies). Geoterm.

Nettletton, L. L. (1942):Gravity and magnetic calculations, Geophysics ***7****, 293–310.*

Peters, L. (1949): The direct approach to magnetic interpretation and its practical application. Geophysics, ***14****, 290–320.*

Plouff D. (1976): Gravity and magnetic fields of polygonal prisms and application to magnetic terrain corrections. Geophysics. ***41****. 727-741.*

Press, W.H., Flannery, B.P., Teukolsky, S.A., Wetterling, W.T. (1986): Numerical Recipes. In: The Art of Scientific Computing, Cambridge University Press.

Rao D. B. and Prakash M.J. (1990): Interpretation of gravity anomalies over an inclined fault of finite strike length with quadratic density function. Exploration Geophysics ***21****, 4, 169-173.*

Roberts R., Hinze W. and Leap D. (1990): Application of the gravity method to the investigation of a landfill in glaciated mid-continent USA: a case study. Geotechnical and Environmental Geophysics ***2,*** *ed S H Ward (Tulsa, USA: Society of Exploration Geophysicists), 253–9.*

Saltus, R. W. and Blakely, R. J. (1983): Hypermag, An interactive, two-dimensional gravity and magnetic modeling program, version 3.5. USGS Open-File Report: 93-287.

Scintrex Ltd. (2012): November 30, 2012 - CG-5 Number 1000. http://www.scintrexltd.com/news/details.php?storeNewsID=11 *visited March 28, 2013.*

Scintrex Ltd. (2012b): CG-5 Operation Manual*.* http://www.scintrexltd.com/dat/content/file/CG-5%20Manual/867700%20_8.pdf *visited March 31, 2013.*

*Silva M. and Andrade A. (1998): On the depth of the hercynian basement in Aveiro region. Comunicacoes do Instituto Geolo gico e Mineiro. Actas do V Congresso Nacional de Geologia, Lisboa, **84**, D40–D43 [in Portuguese].*

*Silva J., Teixeira W. and Barbosa V. (2008): Gravity data as a tool for landfill study. Environ. Geol. **57**, 4, 749-757.*

*Talwani, M., Worzel J. L., and Landisman M. (1959): Rapid gravity computations for two-dimensional bodies with application to the Mendocino submarine fracture zone. J. Geophys. Res., **64**, 1, 49–59.*

Tamura Y. (1987): A Harmonic Development of the Tide Generating Potential. *Bulletin d'informations marees terrestres. **99**.*

Teixeira, C., Zbyszewski, G. (1976): Geological map of Portugal, sheet 16-A, Aveiro, scale 1:50000. Serv. Geol. Portugal, Lisboa [in Portuguese].

*Tsirel, S.V. (1994): Methods of calculating the bulk density of a rock mass. Journal of Mining Science **30**, 1, 30-40.*

Appendices

A. Mantlik F. at all: The use of gravity methods in the internal characterization of landfills—a case study - published in Journal of Geophysics and Engineering, 2009, IF=0.787
B. Mantlik F. and Matias M.: Interpretation and modelling of regional gravity data of the Aveiro Basin (Northwest Portugal) – published in Comptes Rendus Geoscience, 2010, IF=1.708
C. Mantlik F. and Karous M.: Use of gravimetry in detailed geophysical prospection of potential geothermal energy exploration areas: Case studies in the territory of the Czech Republic – submitted to Geophysics, 2013, review process completed in April 2013
D. Mantlik F.: BlueWhaleProcessing Geophysical Software: User’s Guide http://bluewhaleprocessing.com/bwpupdates/installers/Documentation.pdf